ASSESSING THE RELIABILITY OF CURRENT SIMULATION OF THERMOELECTRIC HEAT PUMPS FOR NEARLY ZERO ENERGY BUILDINGS: EXPECTED DEVIATIONS AND GENERAL GUIDELINES

Alvaro Martinez[a,b,*], Sergio Díaz de Garayo[c]; Patricia Aranguren[a,b]; David Astrain[a,b]

a Department of Engineering, Public University of Navarra, 31006 Pamplona, Spain

b Smart Cities Institute, 31006 Pamplona, Spain

c National Renewable Energy Centre, 31621 Sarriguren, Spain

*Corresponding author: alvaro.martinez@unavarra.es

Abstract

This paper makes evident that a rigorous review of simulation methods for thermoelectric heat pumps in nearly-zero energy buildings is needed, as incoherent results during verification and validation of simulation models are reported in the literature. Statistical methods based on uncertainty analysis are deployed to calculate the minimum deviations between experimental and simulated values of the main variables that define the performance of a thermoelectric heat pump, within working scenarios expected in nearly-zero energy buildings.

Results indicate that the narrower confidence intervals of these deviations are set by the uncertainties in the calculation of the thermoelecric properties of the thermoelectric modules. The minimum deviation in the prediction of the electric power consumed by the thermoelectric heat pump is ±6% in all scenarios. Likewise, confidence intervals for the heat flow emitted to the hot reservoir range from ±8% for high operating voltages of the thermoelectric heat pump to ±23% for low ones. In similar terms, those of the coefficient of performance range from ±4% to ±21%. These lower limits cannot be reduced unless the uncertainties in the measurement of the thermoelectric properties are reduced.

In fact, these confidence intervals are due to increase as more uncertainties are added in the analysis, so wider intervals are expected when heat exchangers and complex heat reservoir are introduced in the system. To avoid so, several guidelines for uncertainty reduction are included in the paper, intended to increase the reliability of the simulation of thermoelectric heat pumps. Among them, relevant is the precise account of the aspect ratio in a thermoelectric module, as well as the deployment of temperature and voltage sensors with systematic standard uncertainties lower than 0.3ºC and 0.01V respectively.

The paper demonstrates the relevance of uncertainty propagation analysis in the verification and validation of the simulation models in this field, and underlines how misleading could be just to compare average values of experimental and simulated results.

Keywords

Thermoelectric heat pump; nearly zero energy building; simple model; uncertainty analysis

1 Glossary

Acronyms	
COP	Coefficient Of Performance
HE	Heat Exchanger
HVAC	Heating, Ventilation and Air Conditioning
LPU	Law of Propagation of Uncertainty
nZEB	nearly-Zero-Energy Building
TEM	Thermoelectric module
THP	Heat Pump based on Thermoelectric technology
Variables	
A	Base area (m^2)
b	Systematic standard uncertainty
C	Coverage factor
c	Specific heat ($Jkg^{-1}K^{-1}$)
d	Density (kgm^{-3})
I	Current intensity (A)
K	Thermal conductance in a TEM (WK^{-1})
k	Thermal conductivity ($Wm^{-1}K^{-1}$)
L	Length (m)
N	Number of thermoelectric pairs in a TEM
$\dot{Q}$	Heat flow rate (W)
$\dot{q}$	Volumetric heat flow (Wm^{-3})
R	Electric resistance in a TEM (Ω)
S	Global Seebeck coefficient in a TEM (VK^{-1})
s	Random standard uncertainty
T	Temperature (K)
t	Time (s)
u	Absolute standard uncertainty
V	Electric voltage supplied to a TEM (V)
$\dot{W}$	Electric power supplied to a TEM (W)
X	Independent variable
Y	Dependent variable
Greek letters	
α	Seebeck coefficient (VK^{-1})
γ	Aspect ratio (m)
Δ	Absolute deviation
δ	Relative deviation
ρ	Electrical resistivity (Ωm)
τ	Thomson coefficient (VK^{-1})
Subscripts/Superscripts	
c	Cold end of a TEM
exp	Experimental
h	Hot end of a TEM
Joule	Joule effect
n	n-doped thermoelectric leg
p	p-doped thermoelectric leg
Peltier	Peltier effect
sim	Simulated
Thomson	Thomson effect

1 Introduction

Around one third of the current energy consumption in China, USA and the European Union is directly produced in houses, offices, shops and other buildings, this being mostly based on fossil fuels [1,2]. In line with this, the European Commission promoted in 2010 the Energy Performance of Buildings Directive [3], which enforces the adoption of the nearly-Zero-Energy standard (nZEB) from 2018.

A building constructed under the nZEB standard is expected to present reduced energy consumption by the application of two general strategies [4,5]. The first one involves the reduction of the energy demands for heating, ventilation and air conditioning (HVAC). The second enforces the adoption of renewable-energy systems and heat-recovery technologies. Both strategies represent a promising field for application of heat pumps based on thermoelectric technology (THP).

Regarding the first strategy, a nZEB is expected to require around 90% less energy for HVAC than that demanded by current buildings. This extremely low energy demand will allow the deployment of less-efficient technologies, alternative to vapour-compression systems, at competitive cost, such as the thermoelectric technology. As for the second strategy, renewable-energy applications in nZEBs relate mostly to solar technology, that includes photovoltaic cells for electricity generation and solar collectors for water heating. Thermoelectric systems present effective combination with both, as they can be powered directly by photovoltaic cells without electric-current inverters, and participate in cogeneration systems with solar collectors [6,7].

The basic layout of a THP is presented in Fig. 1. This is composed of a thermoelectric module (TEM) that absorbs heat from a cold reservoir ($\dot{Q}_c$) and emits heat to a hot one ($\dot{Q}_h$), when being supplied with electric power ($\dot{W}$). This is the well-known Peltier effect [8,9]. A TEM is composed of several thermoelectric pairs connected in series by metallic shunts, and sandwiched between ceramic plates that provide electrical insulation. Each pair includes a n-doped and a p-doped semiconductor leg, wherein the electric current acts as working fluid. Consequently, and contrary to vapour-compression systems, a THP presents neither real fluids nor moving parts, thus exhibiting robustness, reliability and virtually no need of regular maintenance. Furthermore, it allows an easy control of heat loads and temperatures, with easy transition from heating to cooling mode. On the other hand, the efficiency of THPs, called coefficient of performance (COP), is significantly lower than that of vapour-compression systems.

It is expected that, under the extremely low energy demand of nZEBs, the cited advantages outweigh the low values of COP. This is the reason why the deployment of THPs for HVAC in nZEBs is a highly promising application that could boost the expansion of this technology. For this to become true, conclusive studies must come out, supported by sound experimental proofs of THPs working under real conditions, as well as accurate simulation models for performance assessment. However, this paper demonstrates in section 2 that current literature on simulation of THPs for nZEBs requires a thorough review, because of incoherent results during verification and validation of simulation models.

This paper sets out to provide a rigorous statistical account of the minimum deviations between experimental and simulated values of the main variables that define the performance of THPs in nZEBs. To do so, section 3 presents the theory background of THP modelling, describing variables and parameters that define the performance of a THP, as well as the statistical procedures involved in the calculation of deviations in their prediction. Then, section 4 describes

the methodology used to estimate the minimum deviations in the simulation of dependent variables, along with the contribution of the independent variables and TEM parameters. The results are presented in section 5 and discussed in section 6. Finally, the main conclusions are introduced in section 7, along with several guidelines intended to reduce deviations and increase the reliability of THP simulation.

2 State of the art on simulation of THPs and THP-based systems for HVAC in nZEBs

The main research lines of THPs in nZEBS contemplate either the deployment of roof/wall/ceiling radiant panels, the thermal management of ventilation airflows or a combination of both strategies [1,2,6,7]. In all of them, THPs present the basic layout of Fig. 1, and work between different heat reservoirs, i.e. inner/outer ambient air, inflowing/outflowing airstreams, phase-change materials, water deposits, etc. Heat exchangers (HEs) are always included between the TEMs and the reservoirs, to increase the COP [10].

The main methods for simulation of a THP found in the literature are four: simple models, analytical models, electric-analogy-based models and numerical models based on finite elements. Among them, the latter approach is regarded as the most reliable and accurate [11], but it entails so high computational cost that its use is constrained to the simulation of a single TEM or very simple systems. In the second place, electric-analogy-based models provide results as accurate as those provided by finite elements, but require much less computational time [11]. These models allow the inclusion of all the thermoelectric effects (Seebeck, Peltier, Joule and Thomson) with temperature-dependant properties, and present simple coupling with HEs and reservoirs. Furthermore, the low computational cost allows the simulation of complete THPs with several components, even for the transient regime. Given all of that, one would expect this approach to predominate in the literature. However, the most-used methodology is the one based on the simple model, which simulates the TEMs with a global thermal balance, assuming constant thermoelectric properties, introduced directly or computed at the TEM mean temperature. These assumptions reduce the simulation to a set of linear equations with straightforward resolution at low computational cost, easily coupled with HEs, reservoirs and other components.

The problem is that accuracy significantly decreases when the simple model is used, thus increasing the deviations between experimental and simulated values of the output variables. In this regard, Fraisse's analytical work [11] reports increasing deviations in the prediction of COP and cooling power for electric current supplied to the TEM higher than 6A, peaking at ±25% for 8A. Martinez's experimental work [12] confirms these results, and reports deviations of ±13% when a Marlow RC12-6 TEM is supplied with 5A. Furthermore, according to the Law of Propagation of Uncertainty (LPU) [13], deviations are expected to increase as the system becomes more complex and additional components are included in the analysis. A simple THP is composed of TEMs and HEs, so deviations coming from HEs simulation combine to those related to TEMs. Similarly, one expects higher deviations in the simulation of systems increasing in complexity, with additional subsystems and changing scenarios.

Consequently, high deviations between simulated and experimental results are expected in the literature related to THPs. This is the case of Shen's work [14], which presents a computational

model for a radiant panel composed of TEMs, a finned heat sink as HE for the hot side of the TEMs, and a flat panel as HE for the cold side. The author uses the simple model for the TEMs and analytically estimated heat transfer coefficients for the HEs, and reports deviations of 30% between simulated and experimental results. Another example can be found in Riffat's work [15], wherein the author presents a THP composed of TEMs, a finned heat sink for the cold side and a heat pipe for the hot side. The increase in complexity comes from the use of a heat pipe, which requires the estimation of several thermal resistances related to heat and mass transfer mechanisms. Consequently, reported deviations are as high as 50% in the COP.

One would expect these results to be predominant in the literature, given the high level of complexity of THPs in nZEBs, but the reality is quite the opposite.

A series of papers have been developed in the Hunan University (Hunan, China) featuring several THP-based systems for HVAC in buildings. Li [16] presents a prototype containing a THP acting over the ventilation system of a building. The THP includes several TEMs and finned heat sinks as HEs, which transfers heat between the airstream flowing in the building and that flowing out. A modified version of this prototype, that includes heat pipes instead of heat sinks, is used to validate a computational model presented by Han [17], which uses the simple model for the TEMs and introduces estimated thermal resistances for the heat pipes. Figures indicate a maximum deviation of 20% between experimental and simulated values of COP, along with a 2.65% (±2ºC) deviation in the temperatures of the airstreams.

In parallel, Liu [18] presents a prototype of an advanced system that combines the previous THP with another THP-based radiant panel, composed of TEMs sandwiched between a flat panel and some heat pipes. This whole system is modelled by Luo [19] with a computational model that includes simple modelling for the TEMs, 2-D heat transfer for the radiant panel, estimated heat transfer coefficients for the thermal contacts, and estimated convective coefficients for the heat pipes. Furthermore, the author indicates that the model is able to simulate the transient state of the system, so the mass and specific heat of all the components are included. Despite the significant increase in complexity, in both the prototype and the computational model, the author reports absolute deviations lower than ±2ºC in the radiant panel and room temperatures.

Further, the model is modified in the TEMs part by including manufacturer's information on temperature-dependent thermoelectric properties, and is subsequently used to design and simulate a THP-based air conditioner with hot water supply [20]. In this design, the TEMs transfer heat between an airstream and a water tank, through HEs with estimated thermal resistances. The simulation includes also the dynamic behaviour of all the components, which the model is able to predict with ±2ºC of deviation in the TEMs temperatures and less than 10% in the COP. Finally, the last improvement proposed by Luo [21] includes 3-D heat transfer for the radiant panel, achieving again a deviation of ±2ºC in the temperatures of the TEMs.

In summary, similar (and minute) deviations in the temperatures are obtained in this series of papers, despite the increasing complexity and the inclusion of dynamic simulation. What is more, deviations in the COP are reduced to the half from the first to the last paper, these being lower than ±10%. Noteworthy is that this outcome is achieved just by the improvement of the simple model, as no improvement in the measurement system is mentioned.

Even more accurate are the simulations reported in Zhao's works. Initially, the author presents a THP for space cooling [22] composed of several TEMs, a finned heat sink for the cold side and a complex system for the hot side. This system includes a water cooling subsystem that transfers heat from the hot side of the TEMs to the ambient air, through either a fin-tube HE or a phase-

change component. In a subsequent paper [23], the author introduces the corresponding computational model, where the TEMs are modelled with the methodology presented by Chen [24]. This methodology is a variation of the simple model that allows the estimation of fixed values for the thermoelectric properties from manufacturer's datasheets. As reported by Chen himself [24], predictions obtained after this modification deviate from those predicted by the simple model. Apart of this new source of uncertainty, the author introduces expressions and estimations for the TEM-to-HE contact and convective heat transfer, TEM-to-water contact and convective heat transfer, 2-D heat conduction in the phase-change material, and conduction-convection heat transfer coefficients for the finned-tube HE. Despite all this complexity, reported deviations in room temperature are within ±0.5ºC.

A similar outcome is reported in Irshad's work [25], where a THP composed of TEMs and finned heat sinks transfers heat between two airstreams. The author presents a model in TRNSYS [26] to simulate the dynamic performance of the system (ventilation, air ducts, HEs and TEMs), including the influence of humidity and temperature varying conditions. The simple model is used for the TEMs, but no mathematical expression is indicated for the rest of the components. Finally, room temperature is predicted with ±0.6ºC of maximum deviation.

To conclude this review, needed is to say that this extraordinary agreement between simulation and experimental data in complex systems with THPs is also present in papers out of the building framework, such as the THP-based cloth dryer presented by Patel [27], or the radiant heating terminal designed by Sun [28].

At this point, one should enquire about the level of reliability of this excellent agreement between experimental and simulated results; in other works, the question is whether the minute deviations reported in the cited literature are expected to occur again when the experiments are replicated. This is the main objective of this paper, as indicated in section 1.

3 Theory background

3.1 Simple model for a TEM in a THP

The conductive heat transfer in a leg of a TEM is given by Eq. (1), where the heat generation rate is governed by the thermoelectric effects. Joule and Thomson effects introduce volumetric heat rates given by Eqs. (2) and (3). Peltier effect introduces local heat rates at either end (heat absorption at the cold end but heat generation at the hot one) given by Eq. (4). Seebeck coefficient, thermal conductivity and electrical resistivity are temperature-dependant; the same occurs with the Thomson coefficient, linked to the Seebeck coefficient by Eq. (5).

$$dc\,{}^{\partial T}/_{\partial t} = \nabla \cdot (k\nabla \mathrm{T}) + \dot{q} \tag{1}$$

$$\dot{q}_{Joule} = \rho\,{}^{I^2}/_{A^2} \tag{2}$$

$$\dot{q}_{Thomson} = \tau\,{}^{I}/_{A}\,{}^{\partial T}/_{\partial \mathrm{X}} \tag{3}$$

$$\dot{Q}_{Peltier} = \pm IT\left(\alpha_p - \alpha_n\right) \tag{4}$$

$$\tau = T\,{}^{\partial \alpha}/_{\partial \mathrm{T}} \tag{5}$$

The simple model assumes 1-D conductive heat transfer with constant properties. Consequently, Thomson effect disappears and heat generated by Joule effect distributes evenly along the legs [11]. The effect of electric contacts and insulation layers is neglected. Heat

extracted from the cold reservoir and that emitted to the hot reservoir are readily calculated by Eqs. (6) and (7) respectively, from which the electric power and the COP are derived. The simple model assumes opposite Seebeck coefficient but equal electric resistivity and thermal conductivity in n-doped and p-doped legs. Likewise, commercial TEMs are designed with legs equal in base area and length, leading to equal aspect ratio.

$$\dot{Q}_c = IT_c^{TEM}S - \left(T_h^{TEM} - T_c^{TEM}\right)K - {I^2R}/{2} \quad (6)$$

$$\dot{Q}_h = IT_h^{TEM}S - \left(T_h^{TEM} - T_c^{TEM}\right)K + {I^2R}/{2} \quad (7)$$

$$\dot{W} = \dot{Q}_h - \dot{Q}_c = VI \quad (8)$$

$$COP = \dot{Q}_h/\dot{W} \quad (9)$$

$$S = N\left(\alpha_p - \alpha_n\right) = 2N\alpha_p \quad (10)$$

$$R = N\left({\rho_p}/{\gamma_p} + {\rho_n}/{\gamma_n}\right) = 2N\,{\rho_p}/{\gamma_p} \quad (11)$$

$$K = N\left(k_p\gamma_p + k_n\gamma_n\right) = 2Nk_p\gamma_p \quad (12)$$

$$\gamma_p = {A_p}/{L_p} = \gamma_n = {A_n}/{L_n} \quad (13)$$

All these equations provide the values of five dependent variables (model outputs), which define the performance of a TEM, namely electric current intensity through the TEM (*I*), electric power consumed by the TEM ($\dot{W}$), heat flow absorbed from the cold reservoir ($\dot{Q}_c$), heat flow emitted to the hot reservoir ($\dot{Q}_h$), and COP.

As model inputs, one finds four TEM parameters, which are the three thermoelectric properties and the aspect ratio of p-doped legs (α_p, ρ_p, k_p, γ_p), along with three independent variables, namely temperatures at the cold and hot side of the TEM (T_c^{TEM}, T_h^{TEM}) and voltage supplied to the TEM (*V*). The independent variables are controlled by the experimenter through the corresponding sensors. Information about the aspect ratio can be extracted from manufacturer's datasheets. The burning point is the introduction of the thermoelectric properties in the model, for which three methods are available.

In the first one, the thermoelectric properties are introduced as temperature-dependant functions computed at the mean temperature of the TEM. The difficulty in obtaining reliable functions makes its use rather scarce in the literature. Recently, Wang [29,30] has provided the most detailed study on the measurement of thermoelectric properties of p-doped bismuth telluride materials used in TEMs from Marlow Industries. Equations (14)-(16) are extracted from these works. The novelty is that this author reports the uncertainties in the calculation of these expressions, which are presented in Section 3.2.2.

$$\alpha_p = -7 * 10^{-6}(T_m^{TEM})^3 + 0.0042(T_m^{TEM})^2 - 0.2862T_m^{TEM} + 106.8 \ \left(\frac{\mu V}{K}\right) \quad (14)$$

$$\rho_p = 0.0094T_m^{TEM} - 1.587 \ \ (m\Omega * cm) \quad (15)$$

$$k_p = 2 * 10^{-5}T(T_m^{TEM})^2 - 0.0131T_m^{TEM} + 3.2025 \ \left(\frac{W}{Km}\right) \quad (16)$$

$$T_m^{TEM} = {\left(T_h^{TEM} + T_c^{TEM}\right)}/{2} \quad (17)$$

As second approach, Chen [24] proposed a method to extract constant values of α_p, ρ_p and k_p from performance parameters of a TEM, provided by the manufacturer. This method regards the TEM as a whole, so the calculated thermoelectric properties include the effect of electrical contacts and insulation layers. However, this method also requires the aspect ratio of a leg for the calculation, which is not always available, so its use is not predominant in the literature.

Finally, the third method was proposed by Lineykin [31], who devised a procedure to extract *S*, *R* and *K* directly from manufacturer's datasheets. Similar to Chen's, the calculation also considers the effect of electrical contacts and insulation layers. Given its simplicity, this is the most used approach.

In this work, the first approach is used, as being the only one whose uncertainty has been calculated according to statistical procedures, and subsequently published [29,30]. Some comments are introduced in section 6 about uncertainty estimation when either Chen's or Lineykin's procedure is deployed.

3.2 Assessing the accuracy of the simple model

To determine how well the model is able to predict the value of a dependent variable (*Y*), one calculates the deviations between simulated and experimental values of this variable, either in absolute (Eq. (18)) or relative (Eq. (19)) terms. Figure 2 shows the procedure followed to obtain these deviations in a TEM simulation; this figure is described in the following paragraphs.

$$\Delta Y = Y_{exp} - Y_{sim} \tag{18}$$

$$\delta Y = {\Delta Y}/{Y_{exp}} = 1 - {Y_{sim}}/{Y_{exp}} \tag{19}$$

3.2.1 Determination of experimental values of dependent variables ($\boldsymbol{Y_{exp}}$)

In the first place, the experimenter sets the values of the three independent variables (*X*, in Fig. 2). As random variables, these are presented by the confidence intervals around the average ($\bar{X}$), including the coverage factor (*C*) and the standard uncertainty (u_X) [13,32]. The latter is determined by the combination of the systematic standard uncertainty (b_X) and the random standard uncertainty (s_X). Random standard uncertainties relate to the person's skill to replicate experiments, so they decrease with increasing number of replications. However, systematic standard uncertainties are related only to the measurement equipment and are not affected by replication. Therefore, they decrease only if the measurement system is improved.

The experimental dependent variables (Y_{exp}) are also random variables, combining average ($\bar{Y}$), coverage factor and standard uncertainty (u_Y). If the dependent variable can be measured directly, the standard uncertainty is determined by the combination of the systematic standard uncertainty (b_Y) and the random standard uncertainty (s_Y). The electric current intensity is an example of this kind, as it can be measured directly with the corresponding sensor. The rest of the dependent variables, though, cannot be measured directly and must be derived from the combination of other measured variables. Then, the corresponding standard uncertainty is obtained by applying the LPU [13]. As an example, the standard uncertainty of the electric power is provided by Eqs. (20) and (21), in absolute and relative terms, obtained after applying the LPU to Eq. (8). The procedure is similar for the rest of the experimental dependent variables.

$$u_{\dot{W}} = \sqrt{I^2(b_V^2 + s_V^2) + V^2(b_I^2 + s_I^2)} \tag{20}$$

$${u_{\dot{W}}}/{\dot{W}} = \sqrt{{(b_V^2 + s_V^2)}/{V^2} + {(b_I^2 + s_I^2)}/{I^2}} \tag{21}$$

3.2.2 Determination of simulated values of dependent variables ($\boldsymbol{Y_{sim}}$)

In the second place, the experimenter introduces in the simple model the same values of the three independent variables to obtain the corresponding simulated values of the dependent variables. The simple model is deterministic, meaning that equal values of the independent variables lead to equal values of the dependent ones. However, dependent variables do also present uncertainty, this coming from the uncertainty of the independent variables and that of the TEM parameters (aspect ratio and the three thermoelectric properties). Therefore, the simulated value of a dependent variable is also a random variable with the corresponding average, standard uncertainty and coverage factor.

Uncertainty in independent variables has been described in 3.2.1. That for the aspect ratio can be extracted from manufacturer's datasheets. Those for the thermoelectric properties are obtained from Wang's papers [29,30], wherein the author provide the data scatter associated with Eqs. (14)-(16). This scatter turns out to be ±4.3%, ±5.0% and ±9.2% for Seebeck coefficient, electrical resistivity and thermal conductivity of the p-doped semiconductor material, within the expected temperature regime of a THP in a nZEB. Then, assuming them to have rectangular statistical distribution, the corresponding standard uncertainties result to be 2.5%, 2.9% and 5.3% for Seebeck coefficient, electrical resistivity and thermal conductivity [32].

The uncertainties in these seven inputs (three independent variables and four TEM parameters) combine via LPU to form the standard uncertainty of each dependent variable. However, no straightforward application of LPU can be done to the set of equations formed by Eqs. (6)-(17). In cases like this, the Monte Carlo method [13] should be applied.

3.2.3 Determination of deviations between experimental and simulated values of dependent variables

Deviations given by Eqs. (18) and (19) depend on experimental values obtained during the testing process and the simulated values provided by the model, for equal input conditions. Since both are random variables, deviations are also random variables, with average and standard uncertainty provided by Eqs. (22) and (23). These expressions make evident that considering only the term of the averages (and neglect that of the uncertainties) for validation and verification of computational models could be highly misleading.

Note also that deviations depend not only on the model accuracy but also on the experimental process deployed to calculate the experimental values. Hence, a highly detailed and precise model might well be spoiled by inaccurate experimental processes with high uncertainty, so special care and detailed information about that should be required from the authors and included in the papers.

$$\Delta Y = \overline{\Delta Y} \pm C u_{\Delta Y} = (\bar{Y}_{exp} - \bar{Y}_{sim}) \pm C \sqrt{u_{Y_{exp}}^2 + u_{Y_{sim}}^2} \tag{22}$$

$$\delta Y = \overline{\delta Y} \pm C u_{\delta Y} = \left(1 - {\bar{Y}_{sim}}/{\bar{Y}_{exp}}\right) \pm C \sqrt{\left({\bar{Y}_{sim}}/{\bar{Y}_{exp}^2}\right)^2 u_{Y_{exp}}^2 + \left({1}/{\bar{Y}_{exp}}\right)^2 u_{Y_{sim}}^2} \tag{23}$$

4 Methodology

This paper sets out firstly to estimate the minimal deviations expected when simulating the performance of THPs with the simple model, and secondly, to assess how these deviations are affected by the uncertainty of the independent variables and TEM parameters. To attain so, the methodology includes the following conditions:

- A single TEM working with a fixed temperature at either end is considered, because such a simple design exhibits the lowest number of sources of uncertainty. The simulation of more complex THPs would surely present higher deviations, as it should include additional uncertainties related to HEs, variable-temperature reservoirs, etc.
- A TEM RC12-6 from Marlow Industries [33] is selected, this being one of the most commonly used in THP applications. Also, Eqs. (14)-(16) and the related uncertainties are obtained from bismuth-telluride specimens of this manufacturer, which ensures the reliability of the results. This TEM presents 127 thermoelectric pairs (245 legs) with aspect ratio of 1.31 mm, derived from a base area of 1.4x1.4 mm^2 and a length of 1.5 mm.
- It is common practice in validation and verification of computational models to introduce correction factors in order to decrease -or even eliminate- the average of the deviations for all the testing points. In this study, the simple model is considered so perfectly corrected that average deviations disappear ($\bar{Y}_{exp} = \bar{Y}_{sim}$) in all the cases.
- The experimental process is considered so perfectly designed that uncertainties related to experimental values ($u_{Y_{exp}}$) are insignificant compared to those of the simulated ones ($u_{Y_{sim}}$). Under these conditions, deviations become minimal as Eqs. (22) and (23) reduce to Eqs. (24) and (25), which present the lowest number of sources of uncertainty.

$$\Delta Y = \pm C u_{Y_{sim}} \tag{24}$$

$$\delta Y = \pm C \, {u_{Y_{sim}}}/{\bar{Y}_{sim}} \tag{25}$$

The following input factors are considered in the analysis, comprising the independent variables and TEM parameters indicated at the top of Fig. 2, along with their standard uncertainties, all of them presented in Table 1. The following paragraphs describe the levels of variation selected for each of them.

- Temperature at the ends of the TEM (T_h^{TEM}, T_c^{TEM}): THPs in nZEBs work in both summer and winter conditions to maintain a comfort temperature inside the building (20 ºC in this study). In summer, the simplest design of a THP extracts heat from the building interior (cold reservoir) and emits heat to the ambient (hot reservoir). The worst considered scenario is shown in Fig. 3a, wherein ambient temperature reaches 40ºC. In winter, the ambient acts as cold reservoir whereas the interior becomes the hot one, the worst scenario being represented by Fig. 3b. Finally, the most favourable conditions occur in summer when ambient temperature equals that of the inside, so the THP must extract only the heat emitted by occupants, machinery, and lighting inside the building. This scenario is presented in Fig. 3c. The temperatures at the ends of the TEMs are selected after considering reasonable temperature gradients in the HEs. Temperature sensors are considered to have systematic standard uncertainty ranging from zero (ideal sensor) to 1.25ºC (non-calibrated sensor with overall uncertainty of 2.5ºC [34]). Random standard uncertainties are neglected.
- Electric voltage (*V*): Commonly, a DC power supply provides the voltage needed by the TEM to operate, varying from 2V in the low range, to the maximum recommended of 14V [33]. An

additional value is taken in the middle range, this being 8V. In the literature, systematic standard uncertainty of voltage sensors varies from zero (ideal sensor) to 0.1V (overall uncertainty of 0.2 V [12,35,36]). Random standard uncertainties are neglected.

- Aspect ratio of 1.31mm is considered in the study, this value coming from the cited dimensions of a leg in a Marlow's RC12-6 TEM. As for the uncertainty, this manufacturer provides a relative standard value of 3.2% in the measurement of the thickness of a TEM [33]. From this, applying LPU to Eq. (13), one finds that the absolute standard uncertainty of the aspect ratio turns out to be 0.04mm. Therefore, in all the scenarios, this uncertainty is allowed to vary from zero (ideal measurement) to 0.04mm.
- Thermoelectric properties: Eqs. (14)-(16) present the expressions for the Seebeck coefficient, electrical resistivity and thermal conductivity of p-doped legs. Their uncertainty is introduced in relative terms, extracted from Wang's papers [29,30], as was described in section 3.2.2.

After the simulation, the model provides the averages and standard uncertainties of the dependent variables shown in the middle of Fig. 2, from which three are selected for analysis and discussion: electric power supplied to the TEM ($\dot{W}$), heat emitted by the TEM to the hot reservoir ($\dot{Q}_h$) and COP. The analysis of the heat flow absorbed from the cold reservoir would be redundant, because it would provide similar results (in terms of uncertainty) to those obtained for the heat flow emitted to the hot reservoir. Likewise, the analysis of the electric current intensity has been neglected because this parameter would present a similar behaviour than that of the electric power.

The analysis focuses on the relative standard uncertainties ($u_Y/\bar{Y}$) of these three variables, providing the minimum values and the influence of all independent variables and TEM parameters. The corresponding confidence intervals for the deviations in the prediction of these variables are therefore formed with Eq. (25). Engineering Equation Solver Professional V9.835 [37], along with its corresponding module for analysis of uncertainty propagation, is used in this study. All variables and parameters are considered normally distributed, except for the thermoelectric properties, which follow rectangular distributions.

5 Results

Table 2 shows the values of the thermoelectric properties (calculated with Eqs. (14)-(16)) used for the three scenarios, along with the absolute standard uncertainties. The relative standard uncertainties displayed in Table 1 have been applied to calculate these absolute standard uncertainties.

5.1 Electric power supplied to the TEM

Results for the electric power supplied to the TEM in all the scenarios are presented in Table 3. Voltage of 2V is removed from the analysis in cold winter and hot summer scenarios, because the TEM is unable to pump heat from the cold to the hot reservoir under these conditions.

Columns from 1 to 3 present the values of TEM temperatures and voltage, whereas columns 4 and 5 show their corresponding absolute standard uncertainty. Column 6 presents the absolute standard uncertainty of the aspect ratio. Finally, columns from 7 to 9 present the average value of the electric power, provided by the simulation, along with the standard uncertainty in absolute and relative terms. See that two cases have been considered for each combination of $\bar{T}_h^{TEM}$, $\bar{T}_c^{TEM}$ and *V*. In the first one, results are calculated taking into account only the

contribution of the uncertainty in the thermoelecric properties, so the uncertainty of temperature, voltage and aspect ratio equals to zero (see columns from 4 to 6). Under these circumstances, the uncertainty in the electric power reaches the minimum values. In the second case, the contribution of the uncertainty of temperature, voltage and aspect ratio is added.

Relative to this, Fig. 4 shows how the uncertainty of each independent variable and TEM parameter contributes to the relative standard uncertainty of the electric power, for the worst summer scenario (top), worst winter scenario (middle) and best scenario (down). Results are duplicated for each voltage, as columns on the left indicate the relative standard uncertainty in the electric power when considering only the uncertainty in the thermoelectric properties, whereas those on the right include also the contribution of the uncertainty in temperature, voltage and aspect ratio.

Global considerations can be extracted, as the results are quite similar for the three scenarios. This could be expected, given that the simple model uses the mean temperature and the temperature difference between the ends of the TEM to compute the electric power, and these are no significantly different in the three scenarios. Therefore, in terms of electric power, and within the temperature framework expected for a THP in nZEBs, the working temperatures of the TEM have no effect on the uncertainty analysis.

In Fig. 4, when only the uncertainty of the thermoelectric properties is considered (columns on the left for each voltage), all relative standard uncertainties in the electric power turn out to be around 3%. This must be considered as the minimum uncertainty that the model could provide on predicting the electric power consumed by a TEM, given the current level of accuracy in the measurement of the thermoelecric properties [29,30]. This value is composed almost exclusively of the uncertainty of the electric resistivity, thus being similar to that (2.9%, see Table 1). The predominance of the Joule effect in Eqs. (6) and (7), especially for high voltages, explains this result. Therefore, a decrease in the uncertainty in the measurement of the electric resistivity would lead directly to a decrease in that of the electric power. The influence of the uncertainty in the Seebeck coefficient slightly appears for low voltages and low current intensities. No effect has the thermal conductivity, because the Fourier's term disappears when Eqs. (6) and (7) are combined to compute the electric power by Eq. (8).

When all independent variables and TEM parameters are considered (columns on the right for each voltage) the relative standard uncertainty in the electric power increases significantly. The uncertainty in the aspect ratio contributes with a 2% in all the cases, being similar to that of the electric resistivity. The problem comes when the uncertainties of voltage and temperatures are considered, especially in the low voltage range, wherein the uncertainty of the electric power soars up to 16%. This is of major relevance, as this value would combine with the experimental uncertainty and coverage factor in Eq. (23) to provide the confidence interval for the deviation in the prediction of the electric power, which might well be as high as ±50% in the simulation of a real THP prototype.

In this regard, Fig. 5 shows how the uncertainty in temperature and voltage measurement influences that of the electric power. Remember from section 4 that u_T= 1.25 and u_V= 0.1 correspond to sensors without further specific calibration. This figure indicates that standard uncertainties lower than 0.3ºC in temperature and lower than 0.01V in voltage are needed to reduce that of the electric power below 5%. For one thing, uncertainty in temperature is always given by the authors in the cited literature, and values lower than 0.3ºC are commonly found. This is not the case of the voltage, whose uncertainty is scarcely provided. In those papers

wherein this information is reported, the uncertainty ranges widely from 0.25% (0.005V for supplied voltage of 2V [38]) to 5% (0.1V for supplied voltage of 2V [39]). Extra care must be taken in the measure of this variable, especially for low power operation of the TEM.

5.2 Heat flow emitted to the hot reservoir

In similar terms to those of the electric power, results for the heat flow transferred from the TEM to the hot reservoir are presented in Table 4. At the same time, Fig. 6 shows how each independent variable and TEM parameter contributes to the relative standard uncertainty of this dependent variable. The analysis is not as simple as that of the electric power, as the pattern in Fig. 6 depends also on the temperature range of the TEM.

If only the influence of the uncertainties of the thermoelectric properties are considered, that of the heat flow varies depending on the size of the three terms that compose Eq. (7). For high voltage (and high current intensity), the term of the electric resistivity predominates, so the uncertainty in the heat flow approaches that of the electric resistivity, the lowest value being 3.5%. For decreasing voltage, the contribution of both the Seebeck coefficient and the thermal conductivity increases, leading to an increase in the uncertainty of the heat flow, with a peak value of 11.6% at 2V. This effect is slightly amplified for larger temperature difference between the ends of the TEM (15ºC in the best scenario; 35ºC in the worst summer scenario; 55ºC in the worst winter scenario).

At this point, interesting is to enquire about the behaviour of the uncertainty for even lower voltages. Calculations with the simple model provide the minimum operating voltage for each scenario that allows heat to be pumped from the cold to the hot reservoir. This voltage is 4.1V in the worst summer scenario; under these conditions, the average heat flow is 4.02W and the relative standard uncertainty reaches 20.2%. In worst winter conditions, the minimum operating voltage is 6.5V, leading to 12.54W of average heat flow and 11.5% of relative standard uncertainty. Finally, in the best scenario, the minimum operating voltage is 1.7V, leading to 1.09W of average heat flow and a surprising relative standard uncertainty of 31.3%.

Luckily, no TEM operates at its minimum voltage in real THPs, so these high values of heat flow uncertainty never take place. In fact, in the best scenario, the uncertainty decreases drastically from 31.3 to 11.6% when the voltage slightly increases from 1.7 to 2V. The same occurs in worst summer conditions, wherein uncertainty decreases from 20.2 to 11.1% when voltage slightly increases from 4.1 to 4.6V.

Therefore, a global conclusion is that the minimum uncertainty that the simple model could provide on predicting the heat flow emitted to the hot reservoir depends significantly on the voltage supplied to the TEM, varying from 3.5% for high voltages to around 11% for those close to the minimum that allows normal operation of the TEM. These values increase when the uncertainties of the rest of TEM parameters and independent variables are included in the analysis. Significant is the influence of the uncertainty of the aspect ratio, which contributes with up to a 2% in the high voltage range, but decreases in relevance for the low range. For this low range, the uncertainties of temperature and voltage sensors become highly relevant, increasing that of the heat flow up to unacceptable values. See that a relative standard uncertainty of 47.1% in the heat flow prediction is obtained for 2V in the best scenario, which would invalidate any simulation conducted with the simple model.

The solution can be found in Fig. 7, which presents the influence of the standard uncertainty of temperature and voltage sensors in that of the heat flow. This figure reports higher

requirements for the temperature sensors, indicating that standard uncertainties lower than 0.2ºC and 0.03V are needed to reduce the uncertainty of the heat flow below 15%, this value being close to the 11.6% obtained when only the uncertainties in the thermoelectric properties are considered.

5.3 Coefficient of Performance

Finally, results for the COP are presented in Table 6, whereas Fig. 8 shows the contribution of each independent variable and TEM parameter to its relative standard uncertainty. Average values of COP are in line with those provided by the literature [6,7], ranging from 1 to 4 depending on the working conditions. The behaviour is similar to that of the heat flow, being highly influenced by the voltage and the temperature regime. This is no surprise, as COP is derived directly from the heat flow by Eq. (9).

Considering only the influence of the thermoelectric properties, one observes that the uncertainty of the Seebeck coefficient predominates for high voltage, leading to relative standard uncertainties of around 2% in COP simulation. For decreasing voltage, the uncertainty of the thermal conductivity gains in relevance, leading to a peak value of 10.4% in the uncertainty of the COP at 2V.

Again, interesting is to calculate the uncertainty in COP for minimum operating voltages. In the worst summer conditions, the relative standard uncertainty of COP turns out to be 18.8% for 4.1V (minimum voltage for normal operation of the TEM), but decreases rapidly down to 9.8% when a voltage of 4.6V is applied. Similarly, in the best scenario, the minimum operating voltage (1.7V) leads to a 30.0% of relative standard uncertainty in the COP, but this decreases drastically to 10.4% when a voltage of 2V is supplied to the TEM. Finally, in the case of the worst winter scenario, the relative standard uncertainty in the COP for the minimum operating voltage (6.4V) is already quite low, this being 10.0%. In conclusion, the minimum uncertainty that the simple model could provide on predicting the COP depends significantly on the operating voltage, varying from 2.0% for high voltages to around 10.4% for voltages close to the minimum that allows normal operation of the TEM.

When the uncertainties of the rest of TEM parameters and independent variables are included, one observes a general increase in the uncertainty of the COP, promoted almost exclusively by that of the temperature sensors. Similar to the previous cases, this increase becomes more evident for low voltages, wherein non-calibrated temperature sensors could lead to unacceptable uncertainties close to 35%. In this regard, Fig. 9 indicates that the deployment of sensors with standard uncertainty lower than 0.3ºC is enough to reduce the uncertainty in the COP down to values close to those obtained when only the uncertainty of the thermoelecric properties is considered (10.4%). Furthermore, there is virtually no influence of the voltage sensor in the uncertainty of the COP.

6 Discussion

The main objective of this paper was to estimate the minimal deviations between experimental and simulated values (provided by the simple model) of the main variables that define the performance of THPs, namely electric power, heat flow emitted to the hot reservoir and COP, in the temperature range expected in nZEBs. It has been detailed in sections 3 and 4 that these minimal deviations take place when the following restrictions are applied:

- Deviations between experimental average values and simulated average values are neglected, as $\bar{Y}_{exp}$ equals $\bar{Y}_{sim}$ in all the cases.
- The contribution of the uncertainty of experimental values ($u_{Y_{exp}}$) is also neglected.
- Random standard uncertainties (s_Y) are neglected in temperature and voltage measurement, so only the systematic term (b_Y) remains.
- A single TEM with fixed temperatures at either end is considered for analysis, in order to eliminate the possible contribution of the uncertainty in the calculation of the thermal resistance of the HEs.

Under these conditions, the confidence intervals of the deviations in the prediction of these dependent variables are given by Eqs. (24) and (25), formed by the combination of the coverage factor and the standard uncertainty of the simulated values provided by the simple model. The uncertainty of three independent variables (voltage and temperature at TEM ends) and four TEM parameters (thermoelectric properties and aspect ratio) contributes to the uncertainty of the simulated values, and in turn, to the confidence intervals of the deviations.

Uncertainty in voltage and temperature measurement can be reduced by the deployment of highly accurate sensors. In fact, it has been demonstrated in section 5 that their contribution becomes insignificant if these sensors present systematic standard uncertainty lower than 0.3ºC and 0.01V respectively. Similarly, the contribution of the uncertainty of the aspect ratio can be virtually eliminated if manufacturers calculate this parameter with lower relative standard uncertainty than that used in this study (3%), and provide this information in the datasheet. Finally, the authors should also put effort in replicate the tests as many times as possible to minimize the contribution of random standard uncertainties. If all these requirements are conducted, the uncertainties in the thermoelecric properties set the minimum uncertainties of the simulated values provided by the simple model, and in turn, the narrower confidence intervals of the deviations. These lower limits cannot be reduced unless the uncertainty in the measurement of the thermoelectric properties decreases. By now, the best outcome is the one presented by Wan [29,30].

Section 5 reports a minimum relative standard uncertainty for electric power of 3% in all the cases, which leads to a ±6% confidence interval in the prediction of this variable. Note that coverage factor of 2 (accounting for a 95% confidence interval) is the most used among engineering applications [13,32]. In similar terms, the confidence interval for the heat flow varies from ±8% to ±23% for decreasing voltage, whereas that of the COP varies from ±4% to ±21%. Note that, in spite of being minimal, these intervals are significant, especially for low voltages. This might be an issue, owing to the fact that a TEM reaches the maximal values of COP when being supplied with low voltage, so many authors recommend the use of this low voltage range in thermoelectric applications [40,41]. Furthermore, these intervals will inevitably increase when the contribution of the uncertainties related to the four restrictions cited at the beginning of this section are included in the analysis. Impossible is to provide a general rule about how these intervals are going to increase, because they will vary from case to case. In this regard, possible scenarios are included in the following paragraphs.

In the first place, the contribution of the uncertainty in the calculation of experimental values ($u_{Y_{exp}}$) might become relevant when dealing with variables such as the COP, whose experimental uncertainty is calculated by the combination of other variables via LPU. As an example, Martinez [12] tested a prototype of a thermoelectric refrigerator and firstly calculated the experimental value of the thermal resistance of the insulation compartment, whose relative

standard uncertainty turned out to be 3.2%. This was subsequently used to calculate the heat flow absorbed by the TEMs, which presented relative standard uncertainty of 4.7%. Finally, the COP was calculated with 5.6% of relative standard uncertainty. This author indicated that three replications sufficed to render random standard uncertainties insignificant compared to systematic ones. If these results of standard uncertainty in the experimental calculation of the COP were added to the simulated ones obtained in this paper, via Eq. (23), the confidence intervals of the deviations in the prediction of the COP would increase, varying now from ±11.9% to ±23.8% for decreasing voltage.

Secondly, it has been assumed throughout this paper that the simple model predicts perfectly the average experimental values, so it presents no deviations between these and average simulated ones. Despite this condition, significant deviations have appeared, as the term of the uncertainty remains in Eqs. (22) and (23). A lot of papers from many scientific fields present verification and validation processes where only the average experimental and simulated values are compared to calculate deviations; needless is to say how misleading this approach might be. On the contrary, this paper has clearly underlined the relevance of uncertainties in the calculation of these deviations.

Therefore, if possible, authors should correct the models to eliminate the average values of the deviations, in order to decrease the confidence intervals. If this cannot be fully conducted, and residual differences remain, Eqs. (22) and (23) must be applied in each testing scenario. An alternative approach is to consider these differences in the averages as a new source of systematic uncertainty, which adds to those of the experimental and simulated standard uncertainties; then, Eqs. (26) and (27) should be applied instead. As an example, if after being corrected, the simple model deviates systematically 5% in the prediction of the COP, Eq. (27) indicates that the confidence interval of the deviations would increase again, now varying from ±15.5% to ±25.8%.

$$\Delta Y = \pm C\sqrt{\left(\bar{Y}_{exp} - \bar{Y}_{sim}\right)^2 + u_{Y_{exp}}^2 + u_{Y_{sim}}^2} \tag{26}$$

$$\delta Y = \pm C\sqrt{\left(1 - {\bar{Y}_{sim}}/{\bar{Y}_{exp}}\right)^2 + \left({\bar{Y}_{sim}}/{\bar{Y}_{exp}^2}\right)^2 u_{Y_{exp}}^2 + \left({1}/{\bar{Y}_{exp}}\right)^2 u_{Y_{sim}}^2} \tag{27}$$

Finally, note that all the papers cited in this work present THPs that include at least a HE at either side of the TEMs. Consequently, temperatures at the ends of the TEM are not independent but dependent variables influenced by reservoirs and HEs. Either calculated by experiments or estimated through expressions in the literature, the thermal resistance of each HE must include the corresponding uncertainty, which combines with those described in this paper. As an example, expressions for convective heat transfer coefficients present uncertainty as high as 20% [42], thus increasing the final uncertainty of dependent variables and the confidence intervals of the deviations.

All this considered, the extraordinary good accordance between experimental and simulated values described in section 1 could hardly be maintained if tests were replicated and/or TEMs were replaced (even with other TEMs of the same kind). Specifically, deviations lower than ±10% are not expected in the simulation of the COP. Special care must be devoted to the experimental

procedures so as not to increase the uncertainties inevitably introduced by the thermoelectric properties.

To conclude, one could enquire what the procedure must be when using Chen's [24] or Lineikyn's [31] approximation for the calculation of the thermoelectric properties, as these are the most used approaches for THP simulation in nZEBs.

In Chen's approximation, constant values of the thermoelectric properties for a p-doped leg (α_p, ρ_p and k_p) are extracted from experimental parameters of a TEM, provided in manufacturer's datasheets. Therefore, the uncertainty in these thermoelectric properties would come from those of the experimental parameters, though this information is never provided. In any case, one could hardly expect this experimental method to lead to lower uncertainties than those provided by Wang [29,30], whose methods were specifically designed to calculate these thermoelectric properties. Therefore, when using Chen's approximation for THP simulation, one should include the standard uncertainties presented in Table 1 for Seebeck coefficient (±2.5 %), electric resistivity (±2.9 %) and thermal conductivity (±5.3 %) of a p-doped leg. Likewise, slightly higher values can be taken as a safety measure.

In Lineikyn's approximation, *S*, *R* and *K* are extracted directly from experimental parameters of a TEM, provided in manufacturer's datasheets, so a similar reasoning to that used for Chen's could be applied. Relative standard uncertainties of these parameters are provided by Eqs. (28)-(30), obtained by applying LPU to Eqs. (10)-(12). If the relative standard uncertainty of the aspect ratio is neglected, the relative standard uncertainty of *S* equals that of the Seebeck coefficient (±2.5%), whereas the relative standard uncertainties of *R* and *K* equal respectively that of the electric resistivity (±2.9%) and that of the thermal conductivity (±5.3 %). If not, slightly higher values can be taken as a safety measure. Again, authors using Chen's or Lineikyn's approximation should correct the models in order to eliminate the average values of the deviations. If not, Eqs. (22) and (23) -or the alternative Eqs. (26) and (27)- should be applied.

$$u_S/S = u_{\alpha,p}/\alpha_p \ \left(\frac{\mu V}{K}\right) \tag{28}$$

$$u_R/R = \sqrt{\left(u_{\rho,p}/\rho_p\right)^2 + \left(u_{\gamma,p}/\gamma_p\right)^2} \ (m\Omega * cm) \tag{29}$$

$$u_K/K = \sqrt{\left(u_{k,p}/k_p\right)^2 + \left(u_{\gamma,p}/\gamma_p\right)^2} \ \left(\frac{W}{Km}\right) \tag{30}$$

7 Conclusions

This paper has made clear that a rigorous account on simulation methods for THP in nZEBs was needed, especially on those methods based on the simple model. Incoherent results during verification and validation of these models make it necessary to conduct a rigorous statistical account to obtain the minimum deviations between experimental and simulated values of the main variables that define the performance of THPs in nZEBs, namely the electric power consumed by the heat pump, the heat flow emitted to the hot reservoir and the COP.

The minimum deviations in all of them occur when only the influence of the uncertainties of the thermoelectric properties are considered. Under these conditions, the narrower confidence interval of deviations in the simulation of the electric power is ±6% for operating voltage close to the maximum allowable by the thermoelecric module, and rises slightly up to ±7% for minimum operating voltage. The uncertainty in the electric resistivity is the major contributor.

For the heat flow emitted to the hot reservoir, the narrower confidence interval of deviations is ±8% for high voltage, increasing to ±23% for low voltage. Again, the uncertainty in the electric resistivity is the major contributor. Finally, the narrower confidence interval of deviations in the simulation of the COP ranges from ±4% for high voltage to ±21% for low voltage. The uncertainty of the Seebeck coefficient is the major contributor.

These confidence intervals set the minimum deviations in the simulation of a THP with the simple model, using the general approach or the methodology proposed by Chen or Lineikyn. These deviations cannot be reduced unless the uncertainties in the measurement of the thermoelectric properties decrease. On the contrary, these intervals are due to become wider when new uncertainties are included in the analysis.

A 3% relative standard uncertainty in the measurement of the aspect ratio has been considered in this study. This additional uncertainty adds four additional points to the reported confidence intervals. Hence, those for the electric power increase up to ±10% and ±12% for high and low voltage respectively, whereas those for the heat flow become ±12% and ±27%. However, the uncertainty in the measurement of the aspect ratio presents no influence in the deviations of the COP. This behaviour is similar in all temperature scenarios expected for THPs in nZEBs. Given that, precise information about this parameter should be required from the manufacturer.

The influence of the uncertainty of temperature and voltage sensors is highly dependent on the voltage range. For high voltage, their influence is negligible. For low voltage, though, the confidence intervals of deviations in electric power, heat flow and COP become unacceptable if non-specifically calibrated sensors are used. In all the cases, these confidence intervals return to minimum values if sensors with standard uncertainties lower than 0.3ºC and 0.01V are deployed.

New sources of uncertainty come with the experimental procedure used to obtain experimental values of electric power, heat flow and COP. These uncertainties become especially relevant when the law of propagation must be applied, so wider intervals are expected as more variables are added in the calculation. The same applies when heat exchangers and complex heat reservoir are introduced in the system. Therefore, impossible is to provide a general rule about how these intervals are going to increase, as they vary from case to case. Detailed description of measurement systems and validation procedures must be requested from the authors, far from the commonly used comparison between average values of experimental and simulated results. In fact, the analysis used in this paper to extract the cited confidence intervals considers that the simple model predicts perfectly the average experimental values, presenting no deviations between these and average simulated ones. In spite of this simplification, significant deviations have appeared, being related only to the uncertainty in the simulation and testing processes.

The correct application of these guidelines will allow the development of conclusive simulation-based studies that, supported by sound experimental proofs, provide reliable assessment on the performance of THPs for HVAC in nZEB. This is the only way to conduct reliable extrapolations and predictions of TPH performance, required to demonstrate the potential of this technology.

Acknowledgements

This work was supported by the Spanish Ministry of Science, Innovation and Universities [grant number RTI2018-093501-B-C22].

References

[1] Liu Z, Zhang L, Gong G, Li H, Tang G. Review of solar thermoelectric cooling technologies for use in zero energy buildings. Energy Build 2015;102:207–16. doi:10.1016/j.enbuild.2015.05.029.

[2] Shen L, Pu X, Sun Y, Chen J. A study on thermoelectric technology application in net zero energy buildings. Energy 2016;113:9–24. doi:10.1016/j.energy.2016.07.038.

[3] EU. Directive 2010/31/EU of the European Parliament and of the Council of 19 May 2010 on the energy performance of buildings (recast). Off J Eur Union 2010:13–35. doi:10.3000/17252555.L_2010.153.eng.

[4] Cuce P, Riffat S. A comprehensive review of heat recovery systems for building applications. Renew Sustain Energy Rev 2015;47:665–82. doi:10.1016/j.rser.2015.03.087.

[5] Li D, Yang L, Lam J. Zero energy buildings and sustainable development implications – A review. Energy 2013;54:1–10. doi:10.1016/j.energy.2013.01.070.

[6] Zuazua-Ros A, Martín-Gómez C, Ibáñez-Puy E, Vidaurre-Arbizu M, Gelbstein Y. Investigation of the thermoelectric potential for heating, cooling and ventilation in buildings: Characterization options and applications. Renew Energy 2019;131:229–39. doi:10.1016/j.renene.2018.07.027.

[7] Irshad K, Habib K, Saidur R, Kareem M, Saha B. Study of thermoelectric and photovoltaic facade system for energy efficient building development: A review. J Clean Prod 2019;209:1376–95. doi:10.1016/j.jclepro.2018.09.245.

[8] Bell L. Cooling, heating, generating power, and recovering waste heat with thermoelectric systems. Science (80-) 2008;321:1457–61. doi:10.1126/science.1158899.

[9] Rowe D. Thermoelectrics Handbook, Macro to Nano. 1st ed. Boca Raton FL: CRC Press; 2006.

[10] Astrain D, Martínez A, Gorraiz J, Rodríguez A, Pérez M. Computational study on temperature control systems for thermoelectric refrigerators. J Electron Mater 2012;41:1081–90. doi:10.1007/s11664-012-2002-0.

[11] Fraisse G, Ramousse J, Sgorlon D, Goupil C. Comparison of different modeling approaches for thermoelectric elements. Energy Convers Manag 2013;65:351–6. doi:10.1016/j.enconman.2012.08.022.

[12] Martínez A, Astrain D, Rodríguez A, Aranguren P. Advanced computational model for Peltier effect based refrigerators. Appl Therm Eng 2016;95:339–47. doi:10.1016/j.applthermaleng.2015.11.021.

[13] Coleman H, Steele W. Experimentation, Validation, and Uncertainty Analysis for Engineers. 3rd ed. Hoboken, NJ: John Wiley and Sons; 2009.

[14] Shen L, Tu Z, Hu Q, Tao C, Chen H. The optimization design and parametric study of thermoelectric radiant cooling and heating panel. Appl Therm Eng 2017;112:688–97. doi:10.1016/j.applthermaleng.2016.10.094.

[15] Riffat S, Ma X, Wilson R. Performance simulation and experimental testing of a novel thermoelectric heat pump system. Appl Therm Eng 2006;26:494–501. doi:10.1016/j.applthermaleng.2005.07.016.

[16] Li T, Tang G, Gong G, Zhang G, Li N, Zhang L. Investigation of prototype thermoelectric domestic-ventilator. Appl Therm Eng 2009;29:2016–21. doi:10.1016/j.applthermaleng.2008.10.007.

[17] Han T, Gong G, Liu Z, Zhang L. Optimum design and experimental study of a thermoelectric ventilator. Appl Therm Eng 2014;67:529–39. doi:10.1016/j.applthermaleng.2014.03.073.

[18] Liu Z, Zhang L, Gong G. Experimental evaluation of a solar thermoelectric cooled ceiling combined with displacement ventilation system. Energy Convers Manag 2014;87:559–65. doi:10.1016/j.enconman.2014.07.051.

[19] Luo Y, Zhang L, Liu Z, Wang Y, Meng F, Xie L. Modeling of the surface temperature field of a thermoelectric radiant ceiling panel system. Appl Energy 2016;162:675–86. doi:10.1016/j.apenergy.2015.10.139.

[20] Liu Z, Zhang L, Gong G, Luo Y, Meng F. Experimental study and performance analysis of a solar thermoelectric air conditioner with hot water supply. Energy Build 2015;86:619–25. doi:10.1016/j.enbuild.2014.10.053.

[21] Luo Y, Zhang L, Liu Z, Wu J, Zhang Y, Wu Z. Three dimensional temperature field of thermoelectric radiant panel system: Analytical modeling and experimental validation. Int J Heat Mass Transf 2017;114:169–86. doi:10.1016/j.ijheatmasstransfer.2017.06.063.

[22] Zhao D, Tan G. Experimental evaluation of a prototype thermoelectric system integrated with PCM (phase change material) for space cooling. Energy 2014;68:658–66. doi:10.1016/j.energy.2014.01.090.

[23] Tan G, Zhao D. Study of a thermoelectric space cooling system integrated with phase change material. Appl Therm Eng 2015;86:187–98. doi:10.1016/j.applthermaleng.2015.04.054.

[24] Chen M, Snyder G. Analytical and numerical parameter extraction for compact modeling of thermoelectric coolers. Int J Heat Mass Transf 2013;60:689–99. doi:10.1016/j.ijheatmasstransfer.2013.01.020.

[25] Irshad K, Habib K, Thirumalaiswamy N, Saha B. Performance analysis of a thermoelectric air duct system for energy-efficient buildings. Energy 2015;91:1009–17. doi:10.1016/j.energy.2015.08.102.

[26] TESS. TRNSYS 2018. http://www.trnsys.com/.

[27] Patel V, Gluesenkamp K, Goodman D, Gehl A. Experimental evaluation and thermodynamic system modeling of thermoelectric heat pump clothes dryer. Appl Energy 2018;217:221–32. doi:10.1016/j.apenergy.2018.02.055.

[28] Sun H, Lin B, Lin Z, Zhu Y, Li H, Wu X. Research on a radiant heating terminal integrated

with a thermoelectric unit and flat heat pipe. Energy Build 2018;172:209–20. doi:10.1016/j.enbuild.2018.04.054.

[29] Wang H, Porter W, Böttner H, König J, Chen L, Bai S, et al. Transport Properties of Bulk Thermoelectrics—An International Round-Robin Study, Part I: Seebeck Coefficient and Electrical Resistivity. J Electron Mater 2013;42:654–64. doi:10.1007/s11664-012-2396-8.

[30] Wang H, Porter W, Böttner H, König J, Chen L, Bai S, et al. Transport Properties of Bulk Thermoelectrics: An International Round-Robin Study, Part II: Thermal Diffusivity, Specific Heat, and Thermal Conductivity. J Electron Mater 2013;42:1073–84. doi:10.1007/s11664-013-2516-0.

[31] Lineykin S, Ben-Yaakov S. Analysis of Thermoelectric Coolers by a Spice-Compatible Equivalent-Circuit Model. IEEE Power Electron Lett 2005;3:63–6. doi:10.1109/LPEL.2005.846822.

[32] Ratcliffe C, Ratcliffe B. Doubt-Free Uncertainty In Measurement. Springer International Publishing; 2015. doi:10.1007/978-3-319-12063-8.

[33] Marlow. RC12-6 2017. http://www.marlow.com/media/marlow/product/downloads/rc12-6-01ls/Rc12-6.pdf.

[34] Ahlborn. T190-0 2017. https://www.ahlborn.com/en_UK/temperature-measurement.

[35] Grelco. GVD 2017. http://grelco.com/wp-content/uploads/2017/10/GVD-en.pdf.

[36] Astrain D, Aranguren P, Martínez A, Rodríguez A, Pérez M. A comparative study of different heat exchange systems in a thermoelectric refrigerator and their influence on the efficiency. Appl Therm Eng 2016;103:1289–98. doi:10.1016/j.applthermaleng.2016.04.132.

[37] F-Chart. Engineering Equation Solver 2017.

[38] Liu Z, Zhang L, Luo Y, Zhang Y, Wu Z. Performance evaluation of a photovoltaic thermal-compound thermoelectric ventilator system. Energy Build 2018;167:23–9. doi:10.1016/j.enbuild.2018.01.058.

[39] Aranguren P, Díaz de Garayo S, Martínez A, Araiz M, Astrain D. Heat pipes thermal performance for a reversible thermoelectric cooler-heat pump for a nZEB. Energy Build 2019;187:163–72. doi:10.1016/j.enbuild.2019.01.039.

[40] Söylemez E, Alpman E, Onat A. Experimental analysis of hybrid household refrigerators including thermoelectric and vapour compression cooling systems. Int J Refrig 2018;95:93–107. doi:10.1016/j.ijrefrig.2018.08.010.

[41] Martínez A, Astrain D, Rodríguez A, Pérez M. Reduction in the electric power consumption of a thermoelectric refrigerator by experimental optimization of the temperature controller. J Electron Mater 2013;42:1499–503. doi:10.1007/s11664-012-2298-9.

[42] Chapman A. Heat Transfer. 4th ed. Prentice Hall; 1984.

FIGURE CAPTIONS

Figure 1. Thermoelectric module (TEM) working as Thermoelectric Heat Pump (THP)

Figure 2. Statistic procedure for determination of deviations between experimental and simulated values of dependent variables of a TEM

Figure 3. Temperatures in a) worst summer scenario; b) worst winter scenario; c) best scenario

Figure 4 – Percentage contribution (∂/∂) of independent variables and TEM parameters to the relative standard uncertainty of the electric power, for worst summer scenario (top), worst winter scenario (middle) and best scenario (down)

Figure 5 – Contribution of the absolute standard uncertainty of temperature and voltage sensors to the relative standard uncertainty of the electric power (best scenario; V=2V; uγ= 0.04mm)

Figure 6 – Percentage contribution (∂/∂) of independent variables and TEM parameters to the relative standard uncertainty of the heat flow emitted to the hot reservoir

Figure 7 – Contribution of the absolute standard uncertainty of temperature and voltage sensors to the relative standard uncertainty of the heat flow emitted to the hot reservoir (Best scenario; V=2V; uγ= 0.04mm)

Figure 8 – Percentage contribution (∂/∂) of independent variables and TEM parameters to the relative standard uncertainty of the COP

Figure 9 – Contribution of the absolute standard uncertainty of temperature and voltage sensors to the relative standard uncertainty of the COP (Best scenario; V=2V; uγ= 0.04mm)

TABLES

Factor	Worst summer scenario	Worst winter scenario	Best scenario
$\bar{T}_h^{TEM}$ (ºC)	50	30	30
$\bar{T}_c^{TEM}$ (ºC)	15	-25	15
u_T (ºC)	Lower level: 0 Higher level: 1.25		
$\bar{V}$ (V)	Lower level: 2	Middle level: 8	Higher level: 15
u_V (V)	Lower level: 0	Higher level: 0.1	
$\bar{\gamma}$ (mm)	1.31		
u_γ (mm)	Lower level: 0	Higher level: 0.04	
$\bar{\alpha}_p(\frac{\mu V}{K})$	$-7 * 10^{-6}(T_m^{TEM})^3 + 0.0042(T_m^{TEM})^2 - 0.2862T_m^{TEM} + 106.8$		
$u_{\alpha,p}/\bar{\alpha}_p$ (%)	2.5		
$\bar{\rho}_p\ (m\Omega * cm)$	$0.0094T_m^{TEM} - 1.587$		
$u_{\rho,p}/\bar{\rho}_p$ (%)	2.9		
$\bar{k}_p\ (\frac{W}{Km})$	$2 * 10^{-5}(T_m^{TEM})^2 - 0.0131T_m^{TEM} + 3.2025$		
$u_{k,p}/\bar{k}_p$ (%)	5.3		

Table 1. Values and levels of variation of independent variables and TEM parameters, and their standard uncertainties

$\bar{T}_h^{TEM}$ (ºC)	$\bar{T}_c^{TEM}$ (ºC)	$\bar{\alpha}_p\ (\frac{\mu V}{K})$	$u_{\alpha,p}\ (\frac{\mu V}{K})$	$\bar{\rho}_p$ $(m\Omega * cm)$	$u_{\rho,p}$ $(m\Omega * cm)$	$\bar{k}_p\ (\frac{W}{Km})$	$u_{k,p}\ (\frac{W}{Km})$
50	15	211.8	5.3	1.285	0.037	1.067	0.057
30	-25	200.4	5.0	1.003	0.029	1.111	0.059
30	15	208.4	5.2	1.191	0.035	1.078	0.057

Table 2 – Values of the thermoelectric properties and their absolute standard uncertainties adopted for each scenario

$\overline{T}_h^{TEM}$ (ºC)	$\overline{T}_c^{TEM}$ (ºC)	V (V)	u_T (ºC)	u_V (V)	u_γ (mm)	$\overline{\dot{W}}$ (W)	$u_{\dot{W}}$ (W)	$u_{\dot{W}}/\overline{\dot{W}}$ (%)
50	15	8	0	0	0	19.64	0.589	3.0
50	15	8	1.25	0.1	0.04	19.64	1.059	5.4
50	15	14	0	0	0	68.09	1.993	2.9
50	15	14	1.25	0.1	0.04	68.09	3.111	4.6
30	-25	8	0	0	0	21.39	0.684	3.2
30	-25	8	1.25	0.1	0.04	21.39	1.222	5.7
30	-25	14	0	0	0	80.63	2.392	3.0
30	-25	14	1.25	0.1	0.04	80.63	3.726	4.6
30	15	2	0	0	0	1.044	0.035	3.3
30	15	2	1.25	0.1	0.04	1.044	0.168	16.0
30	15	8	0	0	0	24.96	0.727	2.9
30	15	8	1.25	0.1	0.04	24.96	1.284	5.1
30	15	14	0	0	0	80.06	2.325	2.9
30	15	14	1.25	0.1	0.04	80.06	3.618	4.5

Table 3 – Average values and uncertainties of electric power supplied to the TEM, provided by the simple model

$\overline{T}_h^{TEM}$ (ºC)	$\overline{T}_c^{TEM}$ (ºC)	V (V)	u_T (ºC)	u_V (V)	u_γ (mm)	$\overline{\dot{Q}}$ (W)	$u_{\dot{Q}}$ (W)	$u_{\dot{Q}}/\overline{\dot{Q}}$ (%)
50	15	8	0	0	0	37.75	1.714	4.5
50	15	8	1.25	0.1	0.04	37.75	2.674	7.1
50	15	14	0	0	0	101.5	3.712	3.7
50	15	14	1.25	0.1	0.04	101.5	5.212	5.1
30	-25	8	0	0	0	27.86	1.789	6.4
30	-25	8	1.25	0.1	0.04	27.86	2.697	9.7
30	-25	14	0	0	0	100.7	3.885	3.9
30	-25	14	1.25	0.1	0.04	100.7	5.398	5.4
30	15	2	0	0	0	3.311	0.386	11.6
30	15	2	1.25	0.1	0.04	3.311	1.559	47.1
30	15	8	0	0	0	55.91	2.085	3.7
30	15	8	1.25	0.1	0.04	55.91	3.216	5.8
30	15	14	0	0	0	124.1	4.284	3.5
30	15	14	1.25	0.1	0.04	124.1	6.066	4.9

Table 4 – Average values and uncertainties of heat flow emitted to the hot reservoir, provided by the simple model

$\overline{T}_h^{TEM}$ (ºC)	$\overline{T}_c^{TEM}$ (ºC)	V (V)	u_T (ºC)	u_V (V)	u_γ (mm)	$\overline{COP}$ (W)	u_{COP} (W)	$u_{COP}/\overline{COP}$ (%)
50	15	8	0	0	0	1,92	0,060	3,1
50	15	8	1.25	0.1	0.04	1,92	0,074	3,8
50	15	14	0	0	0	1,49	0,031	2,1
50	15	14	1.25	0.1	0.04	1,49	0,033	2,2
30	-25	8	0	0	0	1,30	0,065	5,0
30	-25	8	1.25	0.1	0.04	1,30	0,081	6,2
30	-25	14	0	0	0	1,25	0,028	2,2
30	-25	14	1.25	0.1	0.04	1,25	0,030	2,4
30	15	2	0	0	0	3,17	0,330	10,4
30	15	2	1.25	0.1	0.04	3,17	1,101	34,7
30	15	8	0	0	0	2,24	0,050	2,2
30	15	8	1.25	0.1	0.04	2,24	0,061	2,7
30	15	14	0	0	0	1,55	0,028	1,8
30	15	14	1.25	0.1	0.04	1,55	0,030	2,0

Table 5 – Average values and uncertainties of COP, provided by the simple model

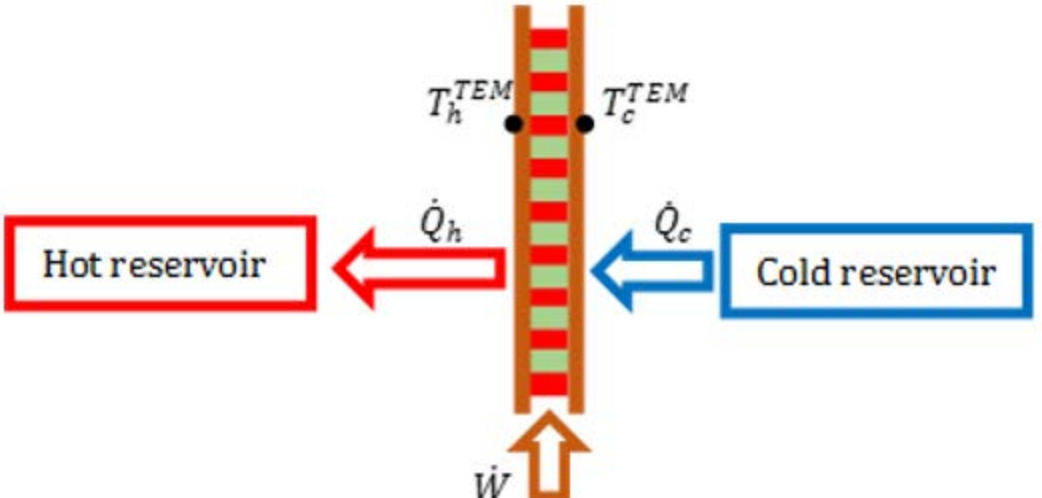
T_h^{TEM}
T_c^{TEM}
$\dot{Q}_h$
$\dot{Q}_c$
Hot reservoir
Cold reservoir
$\dot{W}$

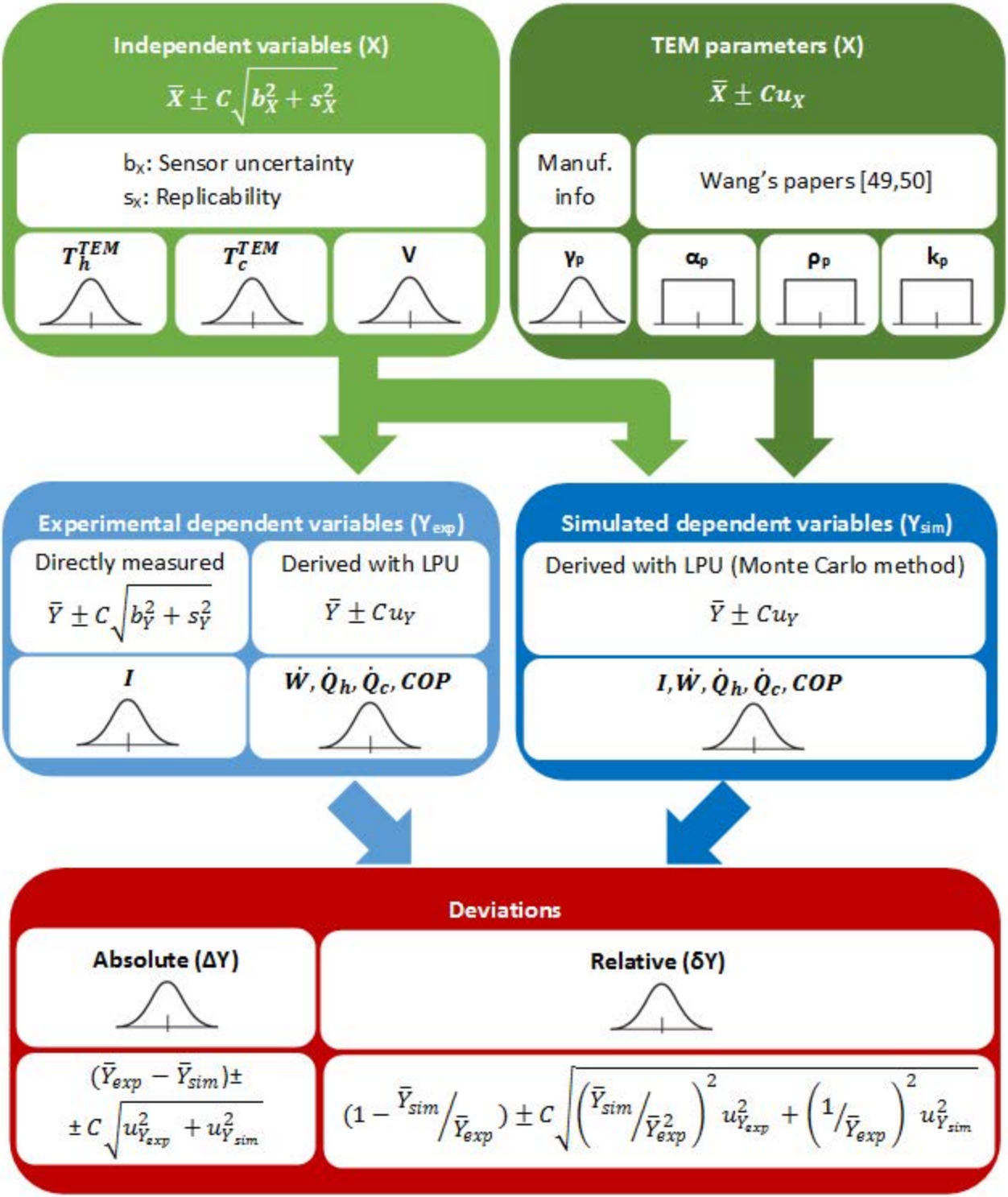
Independent variables (X)
$\bar{X} \pm C\sqrt{b_X^2 + s_X^2}$
b_X: Sensor uncertainty
s_X: Replicability
T_h^{TEM}
T_c^{TEM}
V
TEM parameters (X)
$\bar{X} \pm C u_X$
Manuf. info
Wang's papers [49,50]
γ_p
α_p
ρ_p
k_p
Experimental dependent variables (Y_{exp})
Directly measured
$\bar{Y} \pm C\sqrt{b_Y^2 + s_Y^2}$
Derived with LPU
$\bar{Y} \pm C u_Y$
I
$\dot{W}, \dot{Q}_h, \dot{Q}_c, COP$
Simulated dependent variables (Y_{sim})
Derived with LPU (Monte Carlo method)
$\bar{Y} \pm C u_Y$
$I, \dot{W}, \dot{Q}_h, \dot{Q}_c, COP$
Deviations
Absolute (ΔY)
Relative (δY)
$(\bar{Y}_{exp} - \bar{Y}_{sim}) \pm$
$\pm C\sqrt{u_{Y_{exp}}^2 + u_{Y_{sim}}^2}$
$(1 - \bar{Y}_{sim}/\bar{Y}_{exp}) \pm C\sqrt{\left(\bar{Y}_{sim}/\bar{Y}_{exp}^2\right)^2 u_{Y_{exp}}^2 + \left(1/\bar{Y}_{exp}\right)^2 u_{Y_{sim}}^2}$

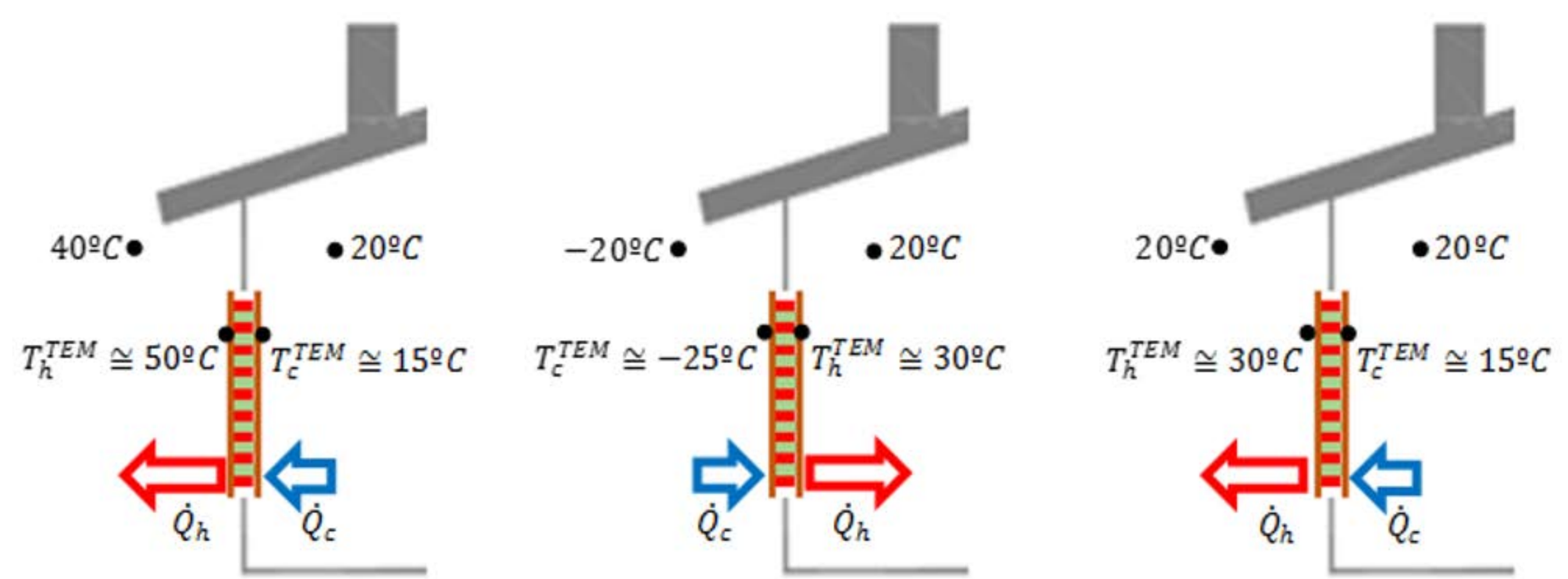
40ºC
20ºC
$T_h^{TEM} \cong 50ºC$
$T_c^{TEM} \cong 15ºC$
$\dot{Q}_h$
$\dot{Q}_c$
−20ºC
20ºC
$T_c^{TEM} \cong -25ºC$
$T_h^{TEM} \cong 30ºC$
$\dot{Q}_c$
$\dot{Q}_h$
20ºC
20ºC
$T_h^{TEM} \cong 30ºC$
$T_c^{TEM} \cong 15ºC$
$\dot{Q}_h$
$\dot{Q}_c$

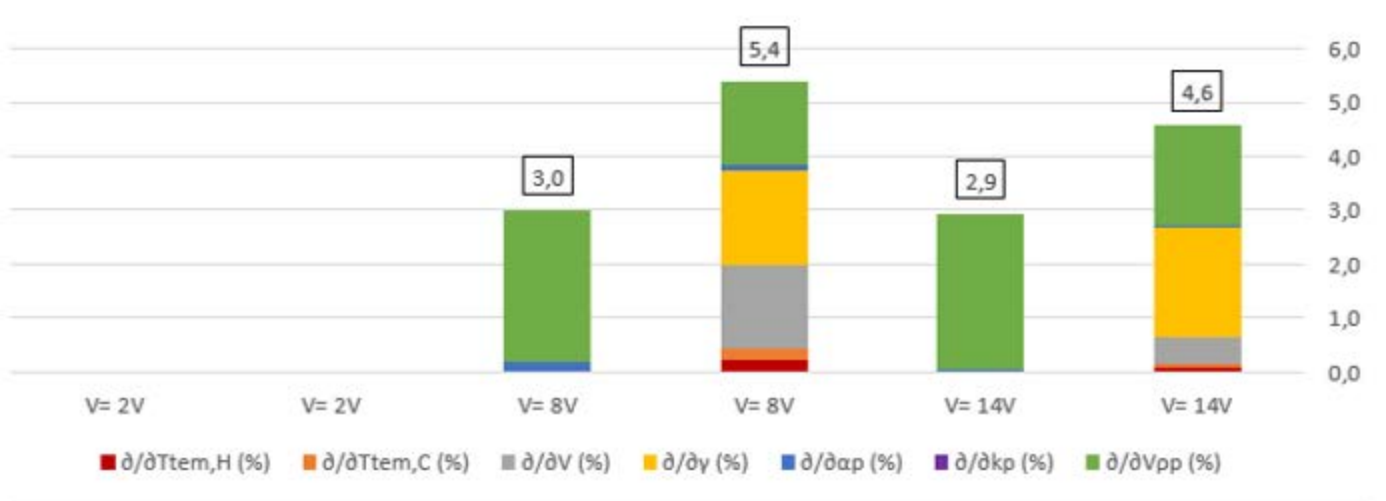
5,4
4,6
3,0
2,9
6,0
5,0
4,0
3,0
2,0
1,0
0,0
V= 2V
V= 2V
V= 8V
V= 8V
V= 14V
V= 14V
∂/∂Ttem,H (%)
∂/∂Ttem,C (%)
∂/∂V (%)
∂/∂γ (%)
∂/∂αp (%)
∂/∂kp (%)
∂/∂Vρp (%)

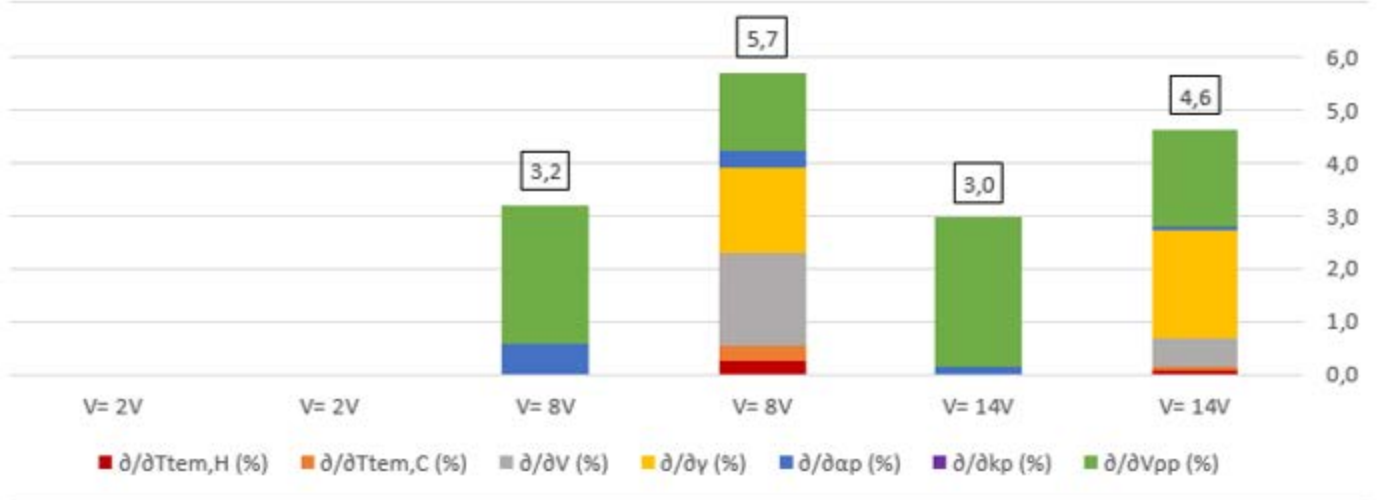
5,7
4,6
3,2
3,0
6,0
5,0
4,0
3,0
2,0
1,0
0,0
V= 2V
V= 2V
V= 8V
V= 8V
V= 14V
V= 14V
∂/∂Ttem,H (%)
∂/∂Ttem,C (%)
∂/∂V (%)
∂/∂γ (%)
∂/∂αp (%)
∂/∂kp (%)
∂/∂Vρp (%)

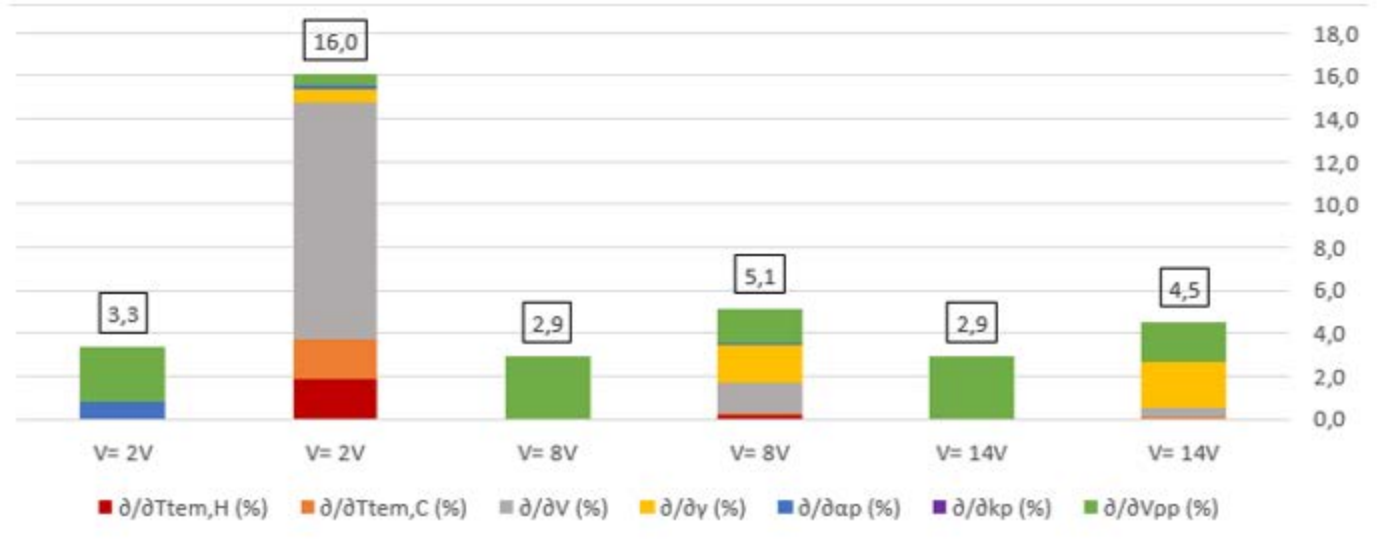
16,0
5,1
4,5
3,3
2,9
2,9
18,0
16,0
14,0
12,0
10,0
8,0
6,0
4,0
2,0
0,0
V= 2V
V= 2V
V= 8V
V= 8V
V= 14V
V= 14V
∂/∂Ttem,H (%)
∂/∂Ttem,C (%)
∂/∂V (%)
∂/∂γ (%)
∂/∂αp (%)
∂/∂kp (%)
∂/∂Vρp (%)

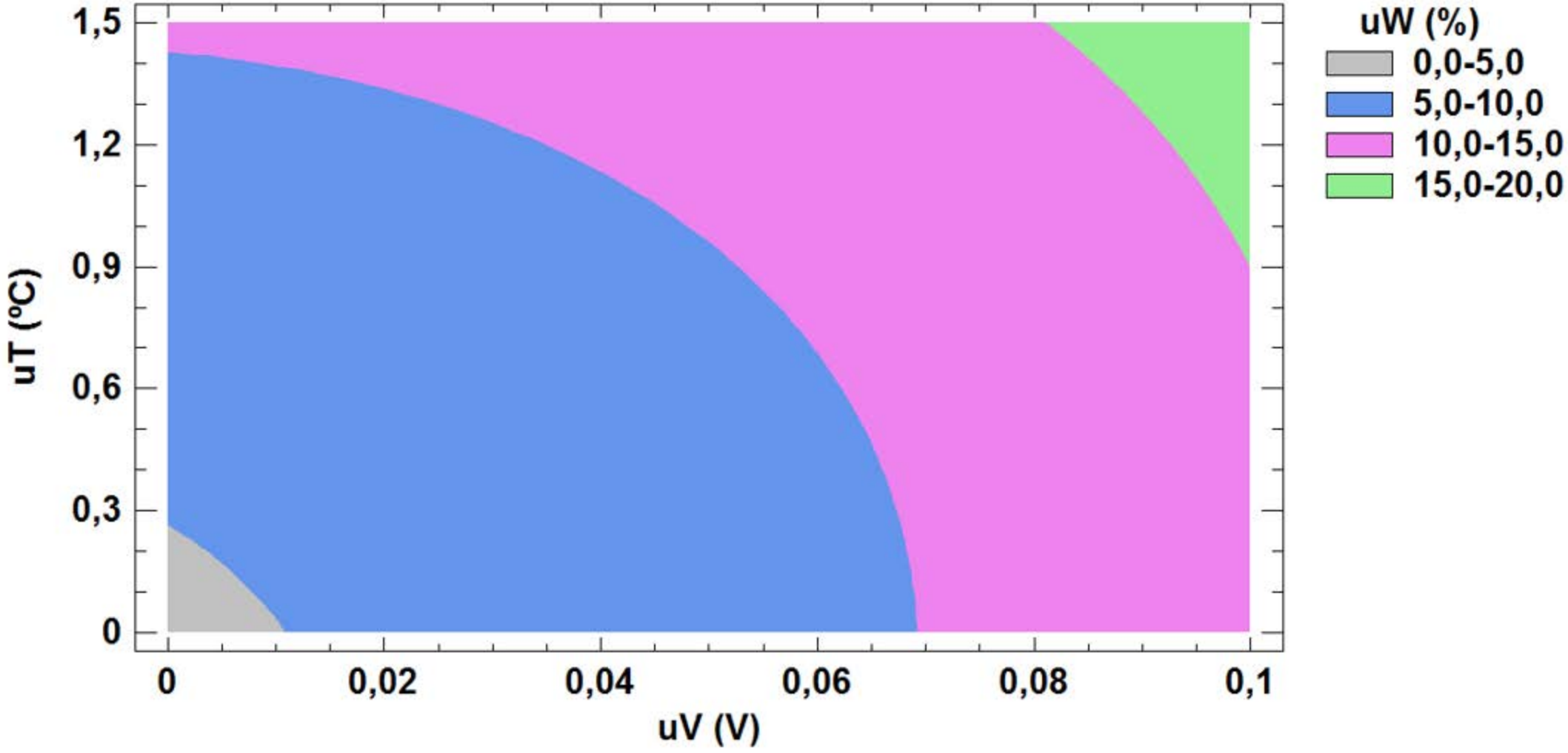
uW (%)
0,0-5,0
5,0-10,0
10,0-15,0
15,0-20,0
uT (ºC)
1,5
1,2
0,9
0,6
0,3
0
0
0,02
0,04
0,06
0,08
0,1
uV (V)

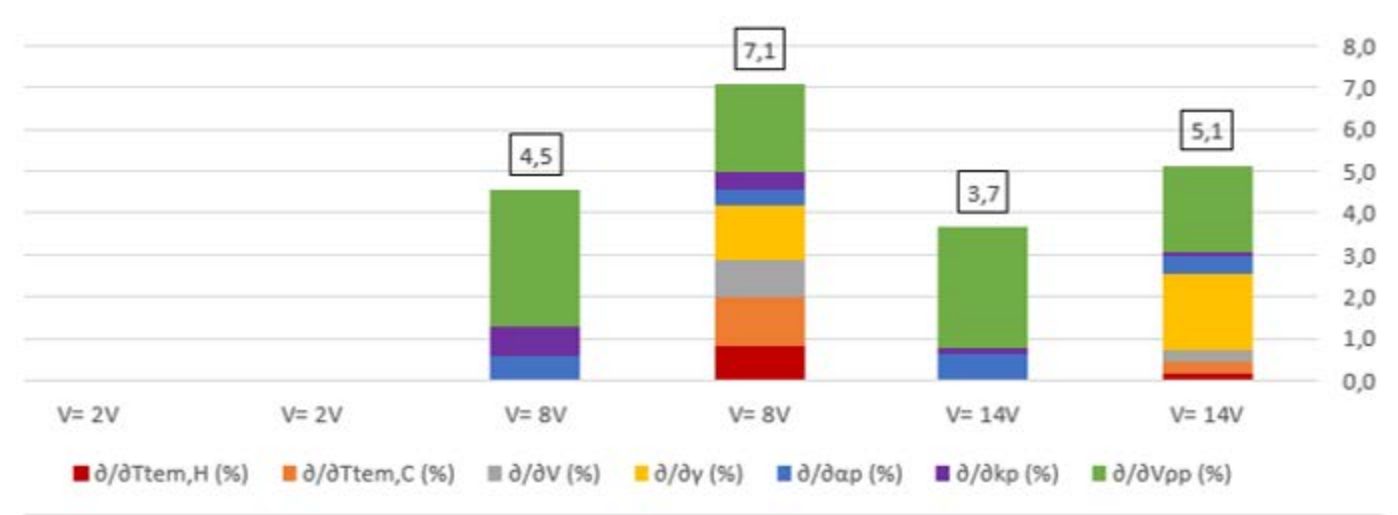
7,1
4,5
3,7
5,1
8,0
7,0
6,0
5,0
4,0
3,0
2,0
1,0
0,0
V= 2V
V= 2V
V= 8V
V= 8V
V= 14V
V= 14V
∂/∂Ttem,H (%)
∂/∂Ttem,C (%)
∂/∂V (%)
∂/∂γ (%)
∂/∂αp (%)
∂/∂kp (%)
∂/∂Vpp (%)

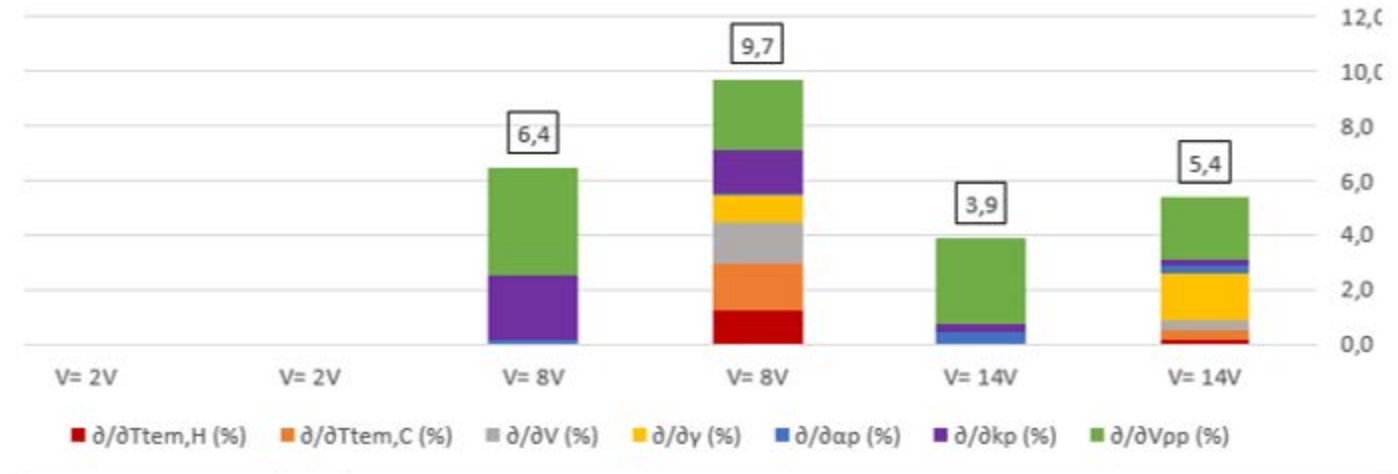
9,7
6,4
3,9
5,4
12,0
10,0
8,0
6,0
4,0
2,0
0,0
V= 2V
V= 2V
V= 8V
V= 8V
V= 14V
V= 14V
∂/∂Ttem,H (%)
∂/∂Ttem,C (%)
∂/∂V (%)
∂/∂γ (%)
∂/∂αp (%)
∂/∂kp (%)
∂/∂Vpp (%)

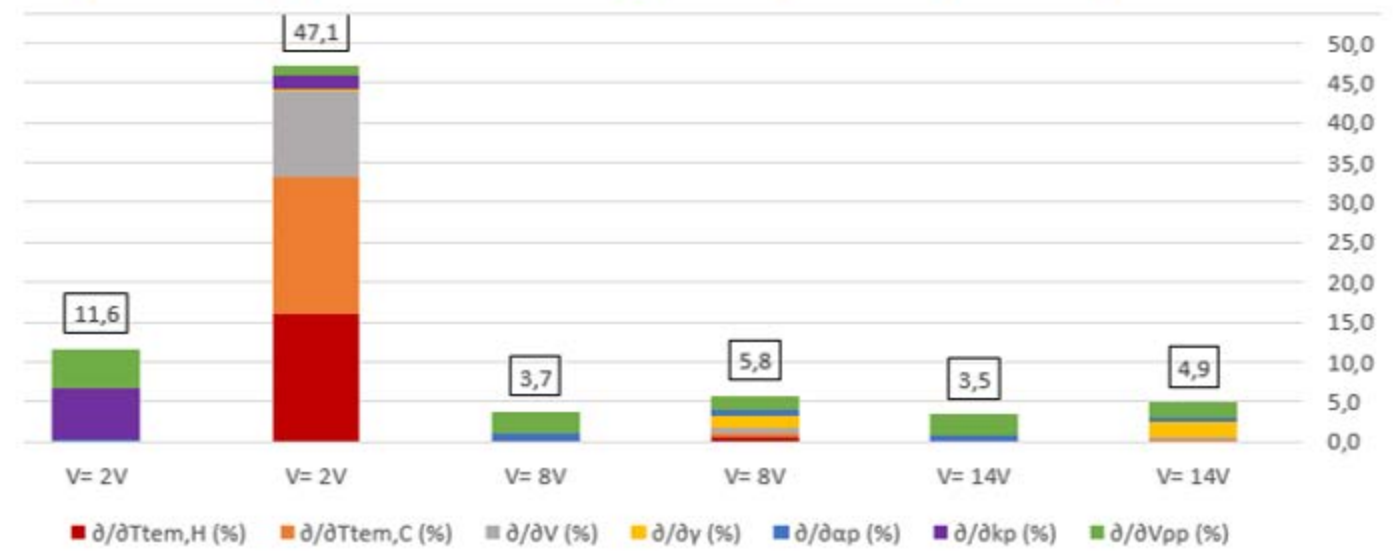
47,1
11,6
3,7
5,8
3,5
4,9
50,0
45,0
40,0
35,0
30,0
25,0
20,0
15,0
10,0
5,0
0,0
V= 2V
V= 2V
V= 8V
V= 8V
V= 14V
V= 14V
∂/∂Ttem,H (%)
∂/∂Ttem,C (%)
∂/∂V (%)
∂/∂γ (%)
∂/∂αp (%)
∂/∂kp (%)
∂/∂Vpp (%)

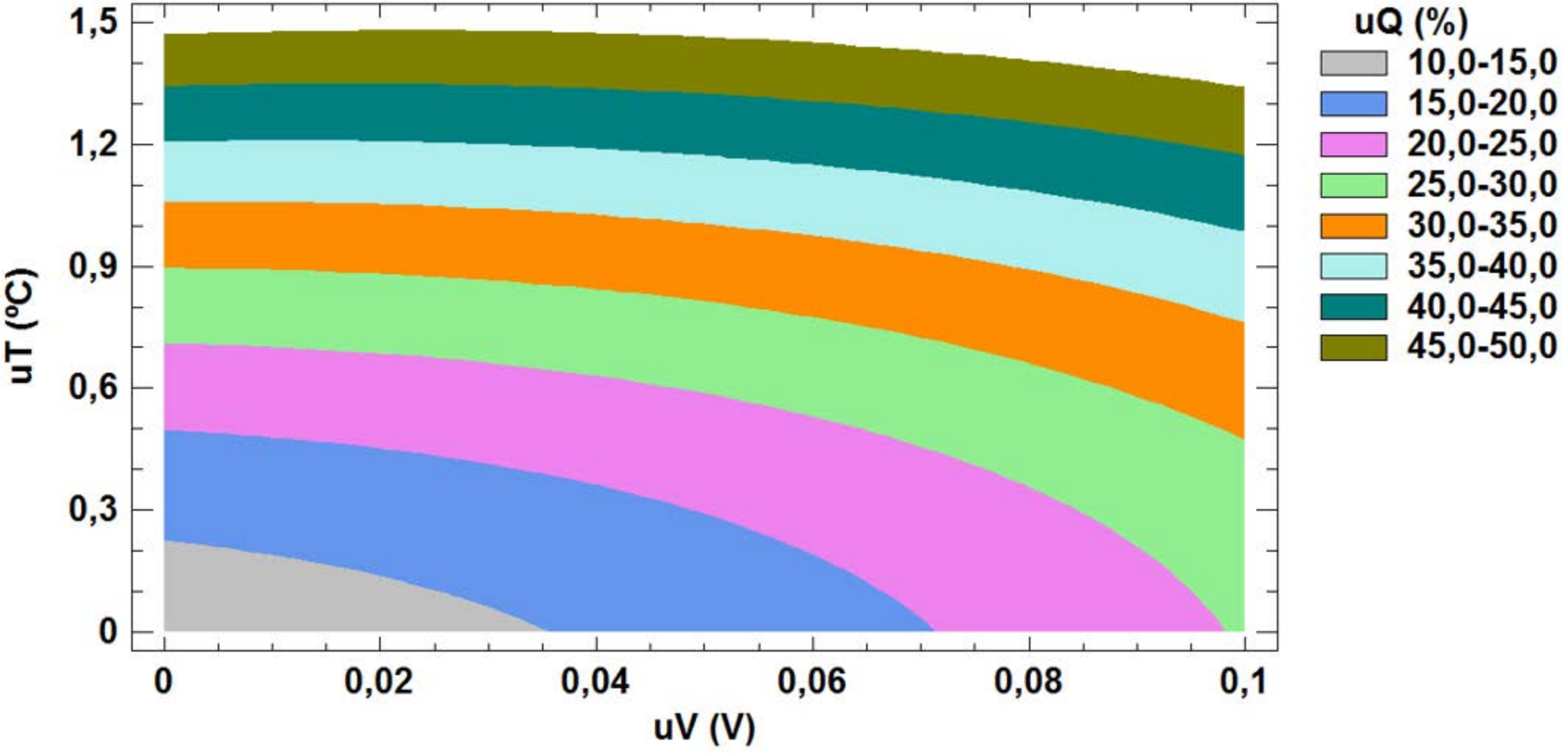
uT (ºC)
1,5
1,2
0,9
0,6
0,3
0
0
0,02
0,04
0,06
0,08
0,1
uV (V)
uQ (%)
10,0-15,0
15,0-20,0
20,0-25,0
25,0-30,0
30,0-35,0
35,0-40,0
40,0-45,0
45,0-50,0

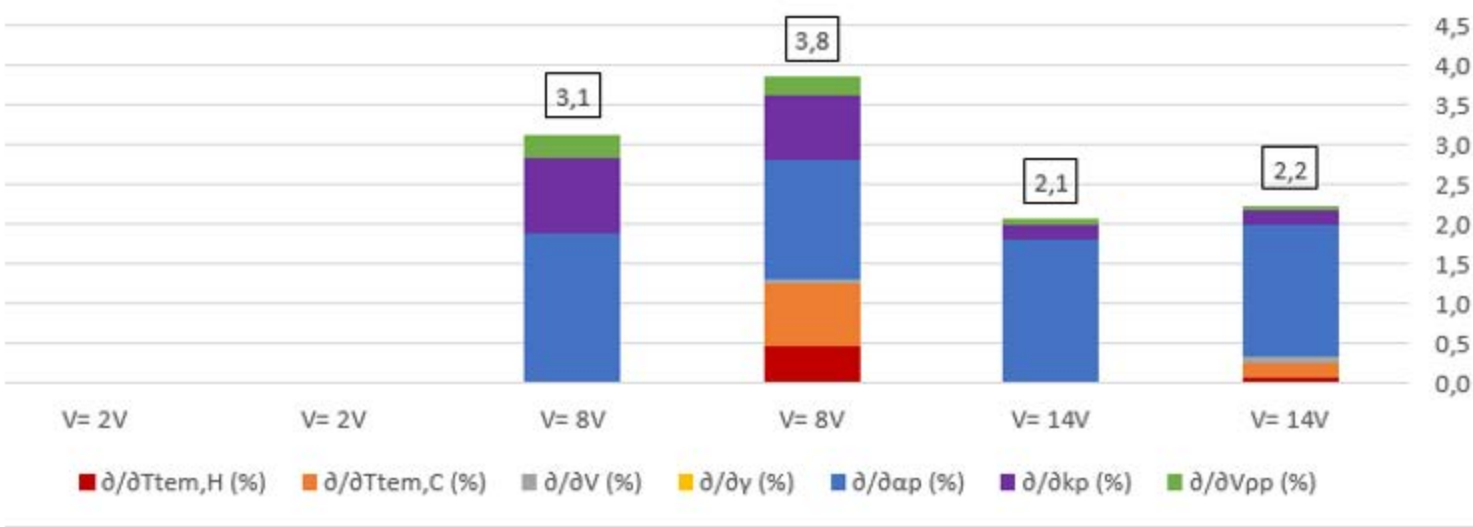
3,1
3,8
2,1
2,2
4,5
4,0
3,5
3,0
2,5
2,0
1,5
1,0
0,5
0,0
V= 2V
V= 2V
V= 8V
V= 8V
V= 14V
V= 14V
∂/∂Ttem,H (%)
∂/∂Ttem,C (%)
∂/∂V (%)
∂/∂γ (%)
∂/∂αp (%)
∂/∂kp (%)
∂/∂Vpp (%)

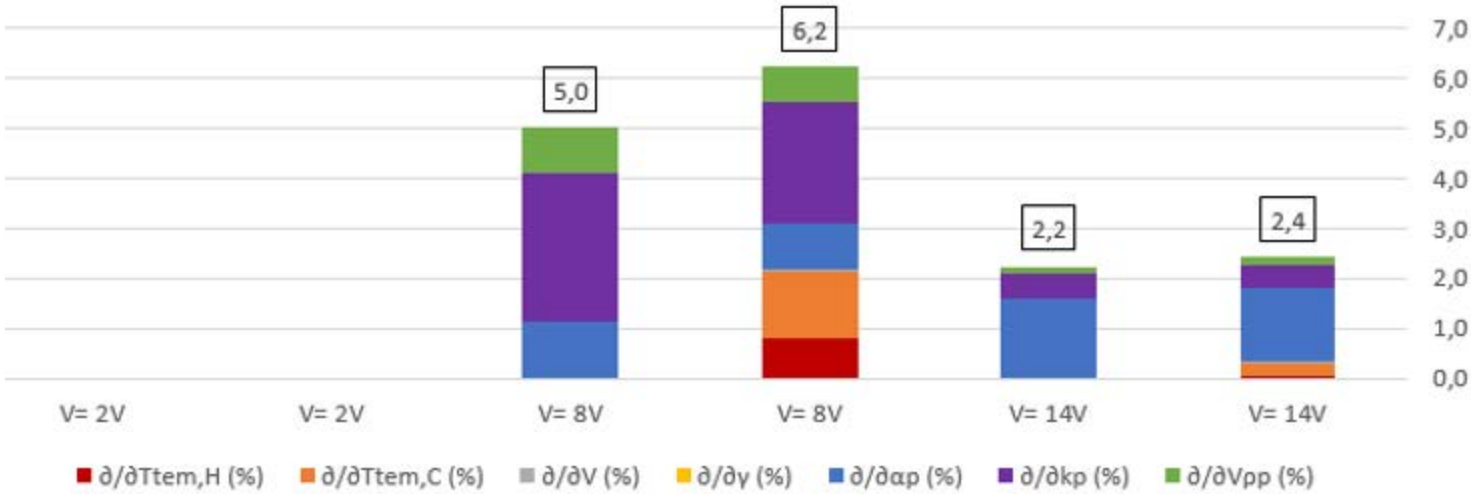
5,0
6,2
2,2
2,4
7,0
6,0
5,0
4,0
3,0
2,0
1,0
0,0
V= 2V
V= 2V
V= 8V
V= 8V
V= 14V
V= 14V
∂/∂Ttem,H (%)
∂/∂Ttem,C (%)
∂/∂V (%)
∂/∂γ (%)
∂/∂αp (%)
∂/∂kp (%)
∂/∂Vpp (%)

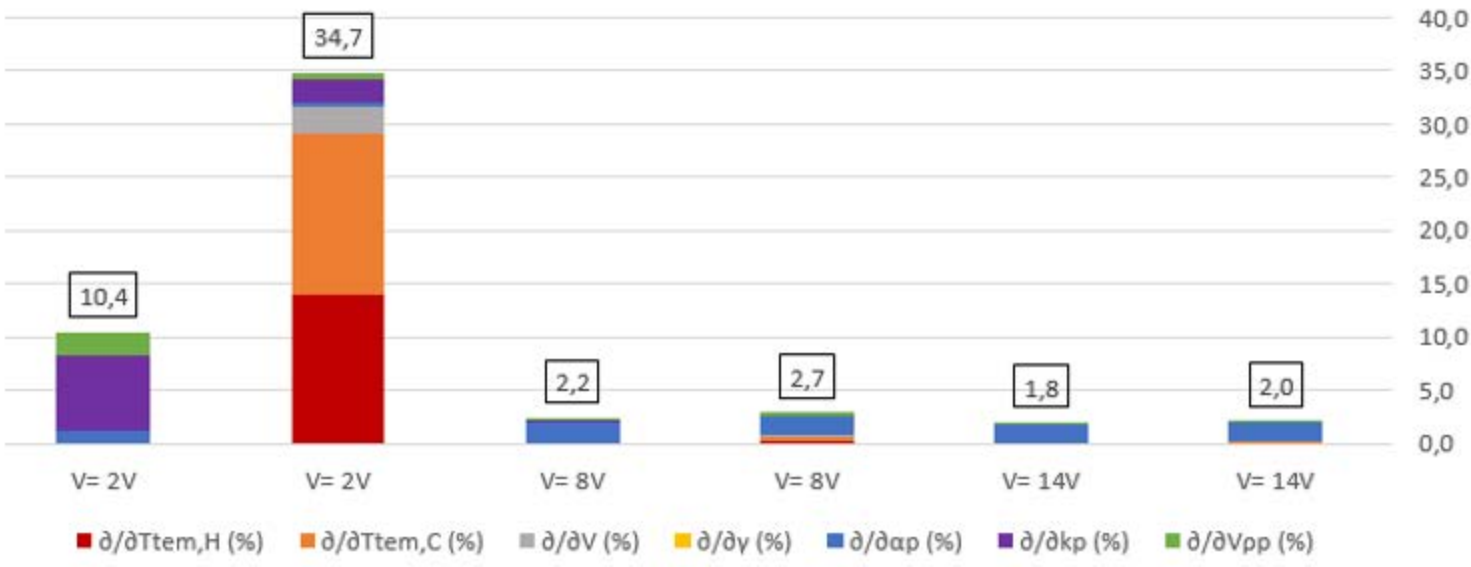
10,4
34,7
2,2
2,7
1,8
2,0
40,0
35,0
30,0
25,0
20,0
15,0
10,0
5,0
0,0
V= 2V
V= 2V
V= 8V
V= 8V
V= 14V
V= 14V
∂/∂Ttem,H (%)
∂/∂Ttem,C (%)
∂/∂V (%)
∂/∂γ (%)
∂/∂αp (%)
∂/∂kp (%)
∂/∂Vpp (%)

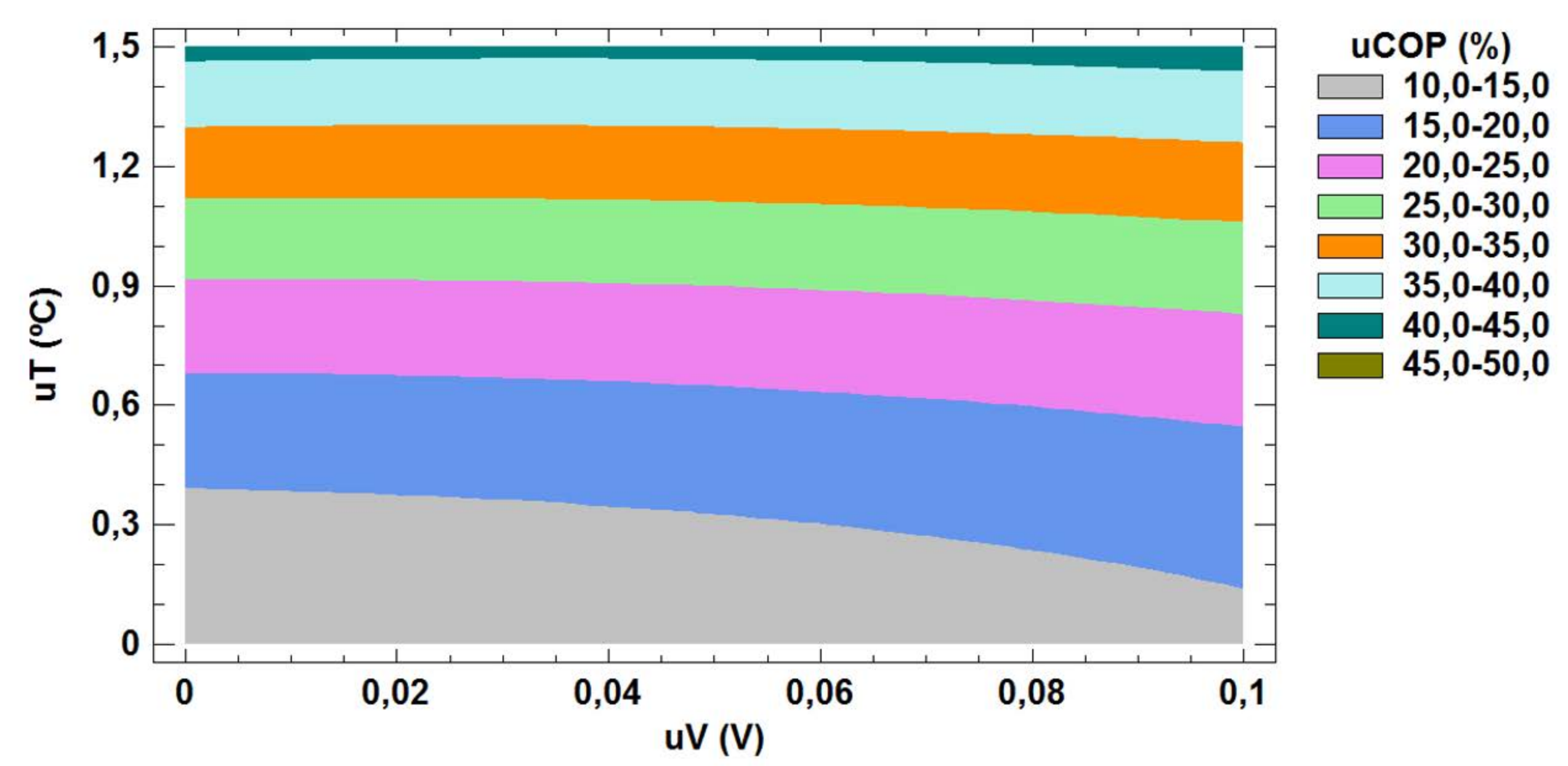
uCOP (%)
10,0-15,0
15,0-20,0
20,0-25,0
25,0-30,0
30,0-35,0
35,0-40,0
40,0-45,0
45,0-50,0
uT (ºC)
1,5
1,2
0,9
0,6
0,3
0
0
0,02
0,04
0,06
0,08
0,1
uV (V)